CHAPTER IV
RESULTS

4.1 Short-term effects of estradiol and CHE on the spatial reference memory of ovariectomized rats

4.1.1 Morris water maze (MWM) test

The time to the platform of the MWM test (mean±SEM) of each group before OVX is shown in Figure 10 (Appendix, Table 2). There was no significant difference between the pre-training 6 groups of animals, so their memory of the platform location was set at the same initial level.

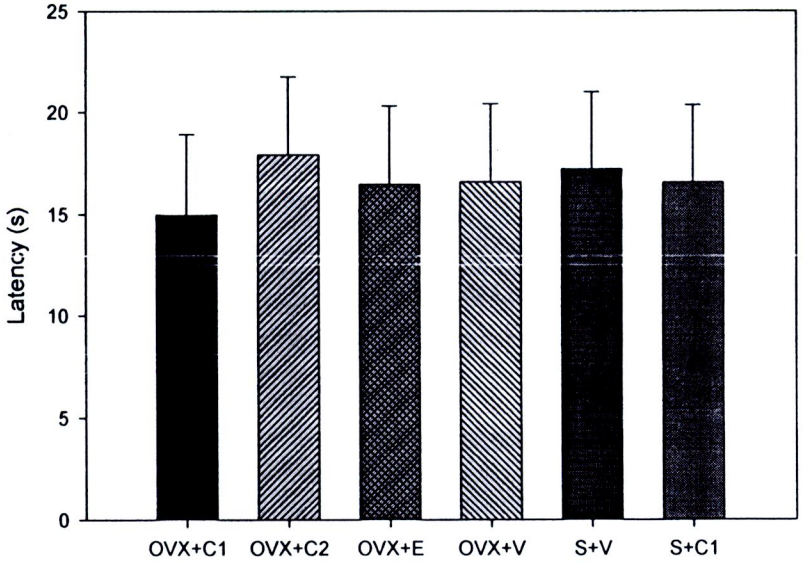

Figure 10 The time to the platform (Mean±SEM) of each groups before OVX. There was no significant difference between groups (ANOVA, P>0.05).

The average time to the platform of the 4 trials in the test day at 1 week, 2 weeks and 4 weeks after OVX are shown (Figure 11) (Appendix Table 2). There was no statistical difference between groups. All the OVX groups had the tendency to increase the latency from 1 week to 4 weeks when compared to the sham ovariectomized groups. The estrogen replacement did not overcome the effect of the OVX to decrease the time to the platform. OVX+C1 and OVX+C2 had the highest

score dispersed away from others along the test except that OVX+C2 increased their performance to shorten the time to find the platform at the test of 2 weeks after OVX. CHE at low dose treatment on the shamed ovariectomized rats did not affect the latency as it did on the OVX rats.

To avoid the interferer of learning ability from one trial to another trial at the tested day, the 1st trial at the 1 week, 2 weeks and 4 weeks were compared (Figure 12, Appendix Table 3). The OVX rats showed the impaired memory at the 2nd week and become the slowest group to reach the platform. Estrogen treatment did not decrease the time but increase the time to the platform. CHE had the similar effect to that of estrogen but in a less level. The high dose of CHE decreased the time to the platform of the OVX rat at the 2nd week, which was similar to the data of the average of 4 trials.

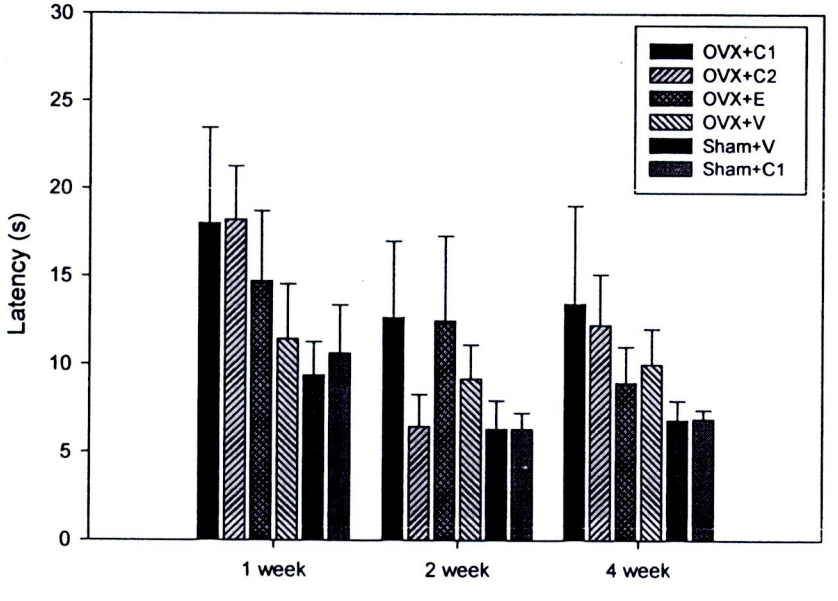

Figure 11 The latency (Mean±SEM) of average of 4 trials at 1 week, 2 weeks and 4 weeks after OVX. There was no significant difference between the groups (ANOVA, P>0.05).

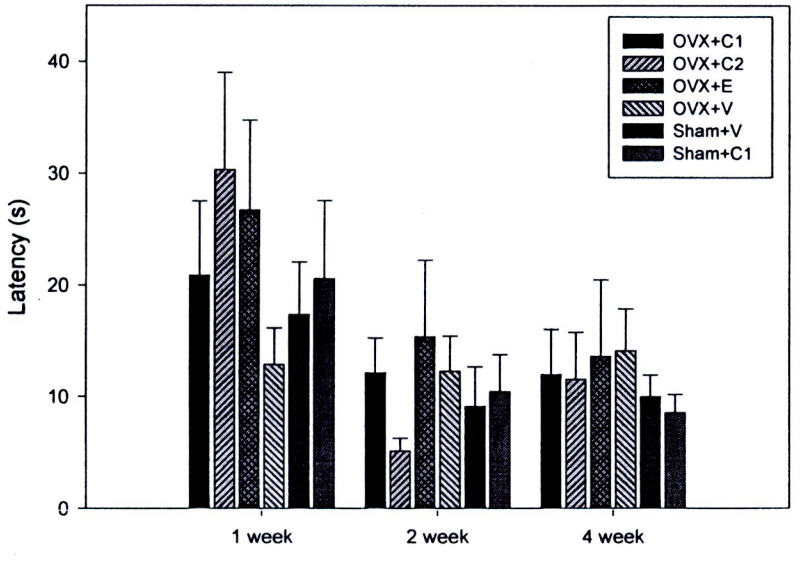

Figure 12 The time to the platform (Mean+SEM) of the 1st trial of each group at 1 week, 2 weeks and 4 weeks after OVX. There was no statistical significant difference between the groups (P>0.05).

4.1.2 Body weight and uterus weight

The surge of the body weight and the significant decrease of the uterus weight of the OVX group indicated the success of the ovariectomized surgery. Estrogen replacement and both doses of the CHE administration reversed these effects in the OVX rats (Figure 13-14) (Appendix Table 4-5).

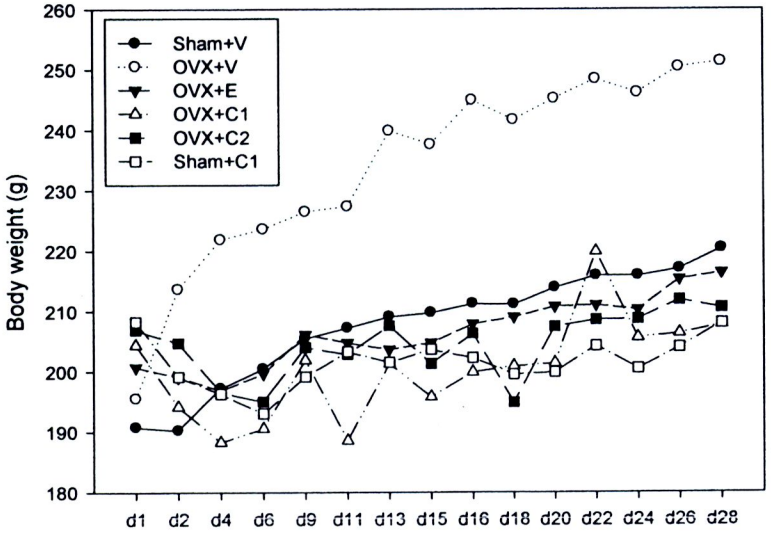

Figure 13 The mean body weight recorded from the day of OVX to the end of short-term behaviors study.

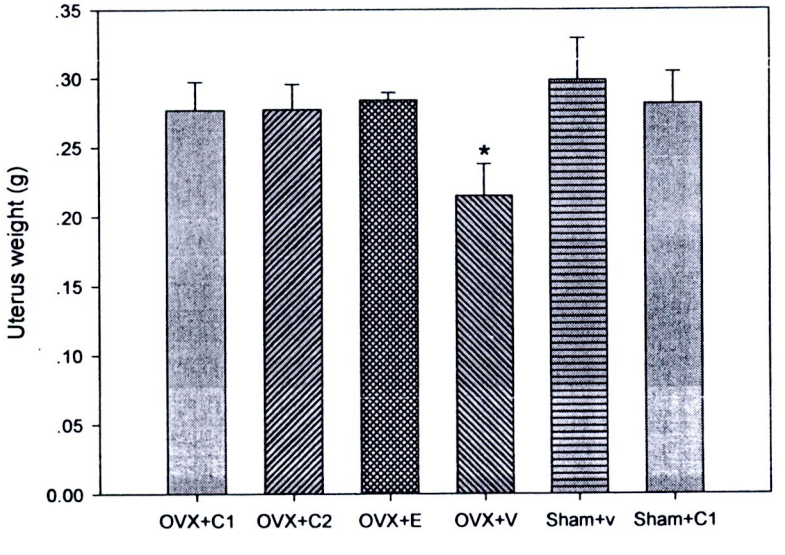

Figure 14 The uterus weight (Mean±SEM) of each group in the short term behavior study.

* Significant different from to the Sham+V, OVX+E and Sham+C1 groups ($P<0.05$).

4.2 RT-PCR quantification of the estrogen receptor mRNA in the hippocampus of the rats.

The hippocampus estrogen receptor alpha, beta and GAPDH mRNA RT-PCR amplified results are shown in Figure 15. As shown in Figure 16-17 (Appendix Table 6), OVX+V group only did not show statistical significant difference to the Sham+V or Sham+C1 groups on both ER alpha and beta mRNA concentrations ($P>0.05$). The estrogen replacement significantly increased both ER alpha and beta mRNA. The administration of CHE increased the ER alpha but not beta mRNA concentrations and the increasing effect was dose-dependent.

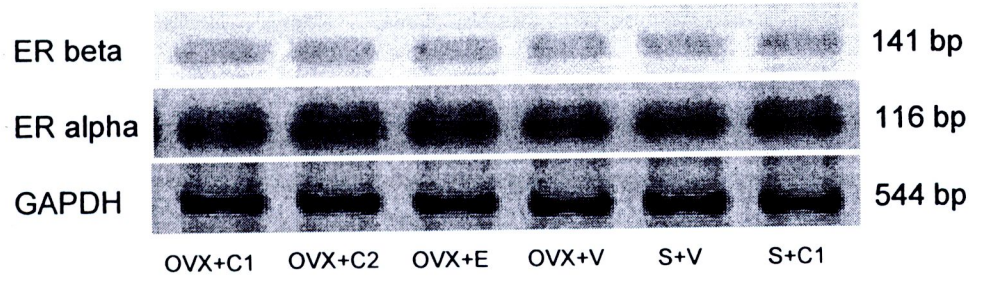

Figure 15 The RT-PCR of hippocampal ER alpha and ER beta mRNA and GAPDH of each group.

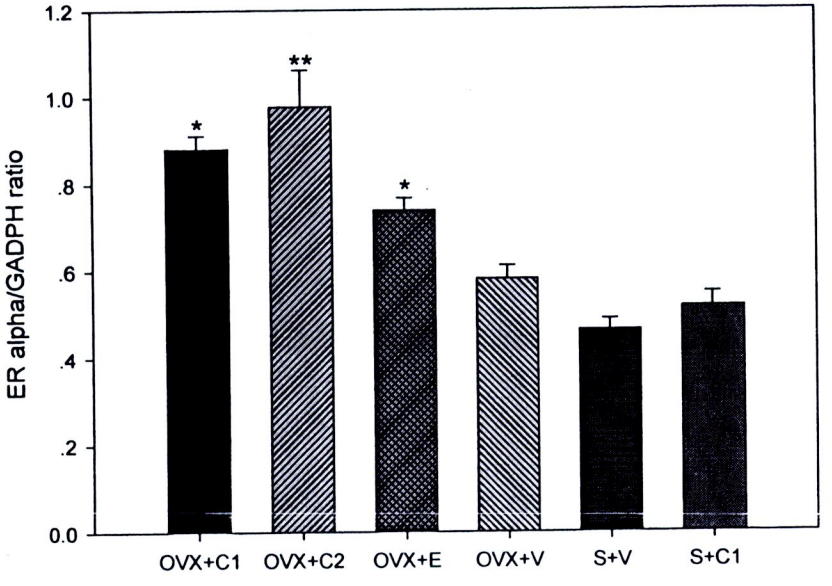

Figure 16 ER mRNA concentration (Mean±SEM) in hippocampus of 6 groups

* Significant different to OVX+V, S+V and S+C1 groups ($P<0.05$).

** Significantly different to OVX+V, S+V, OVX+E and S+C1 groups ($P<0.05$).

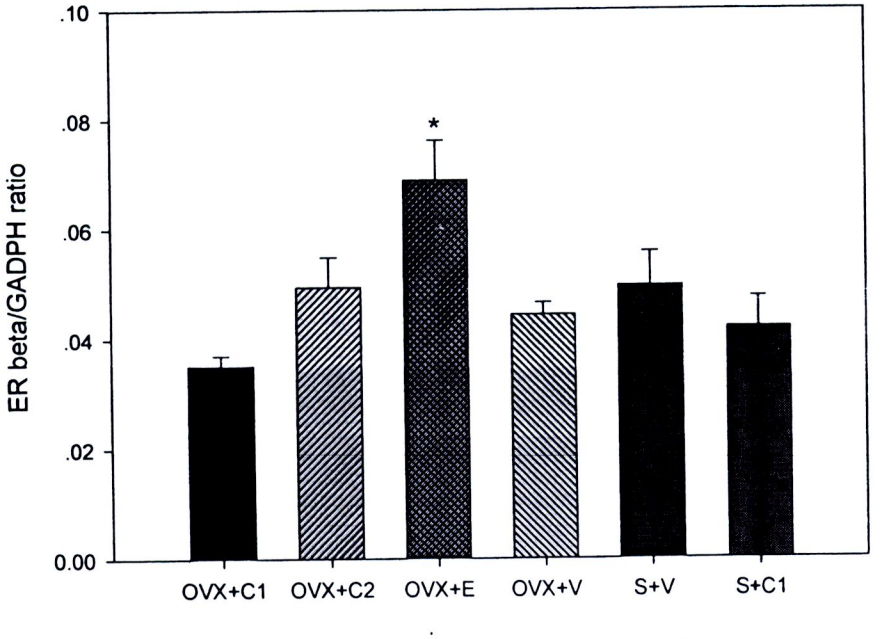

Figure 17 ER beta mRNA concentration (Mean±SEM) in hippocampus of 6 groups

* Significantly different from the other 5 groups ($P<0.05$)

4.3 Long-term effect of estradiol and CHE on the spatial reference memory and working memory of the ovariectomized rats

All the data are also shown in the Appendix, Table 7-26. The swimming traces in the swimming pool of the animals were recorded and the patterns of the tracks of the good memory or impaired memory animals are shown in Figure 18.

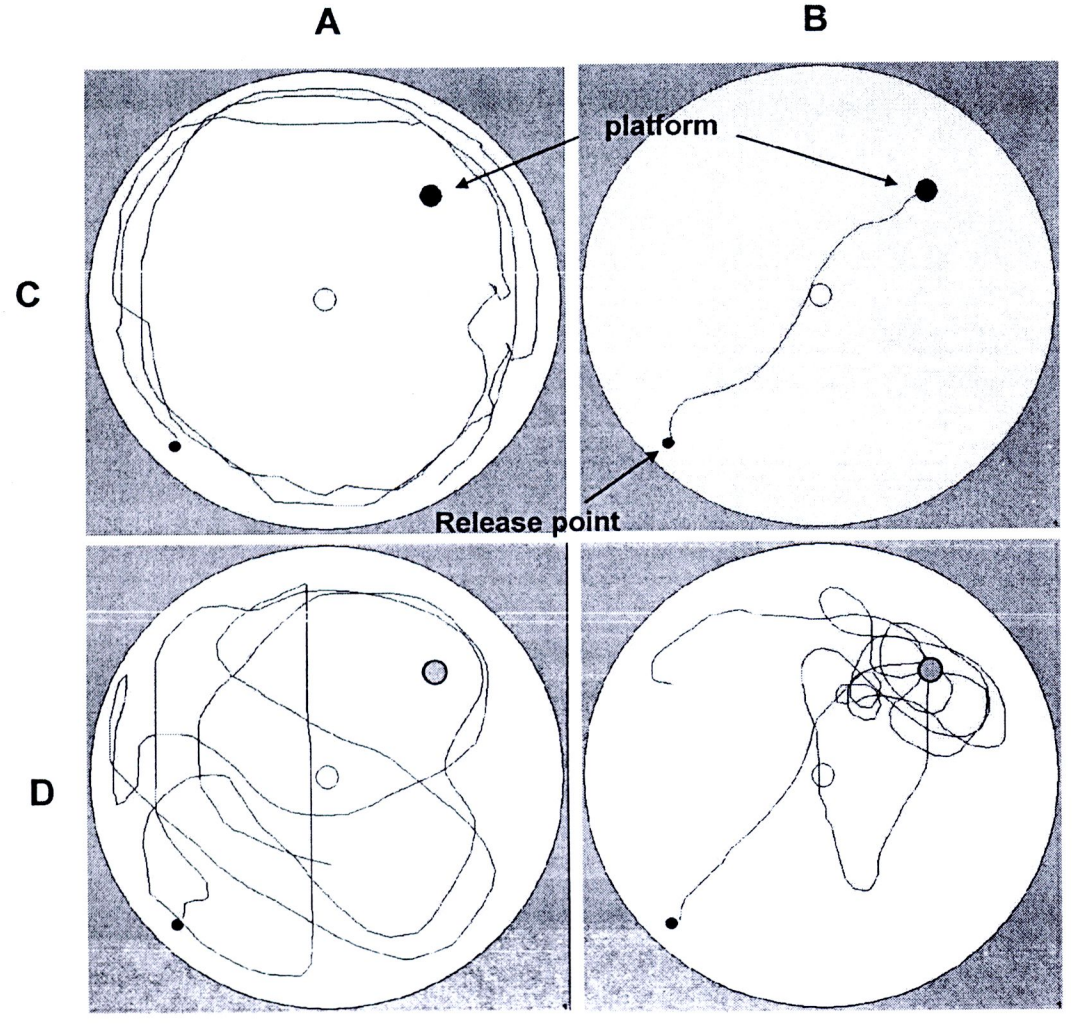

Figure 18 The swimming track of the animal at the MWM test. A: animal with impaired memory; B: animal with good memory; C: the hidden platform test; D: probe test.

4.3.1 MWM test

a) The 1st period

At the 1st period hidden platform test (M-H1), with the platform located in the NE quadrant, the time and distance spent to find the platform for all animal

groups decreased across the 5 testing days, which indicated the increased memory progress of platform location. The effect of CHE was observed at the 3rd day, while OVX+C2 group had the fewer time and shorter distance to find the platform compared to OVX+V and OVX+C1 groups (Figure 19-20). At the 5th day, OVX+C2 group showed a fewer swimming path parallel to the wall the OVX+V group (Figure 21), indicating more efficient path to reach the platform of the OVX+C2 group.

At the probe test (M-P1) 30 days later, the OVX+C2 group had a longer time spent in the NE quadrant (current goal quadrant) when compared to the other 4 groups, indicating a better spatial reference memory (Figure 22).

The OVX+V group did not show poor performance to find the platform in both M-H1 and M-P1.

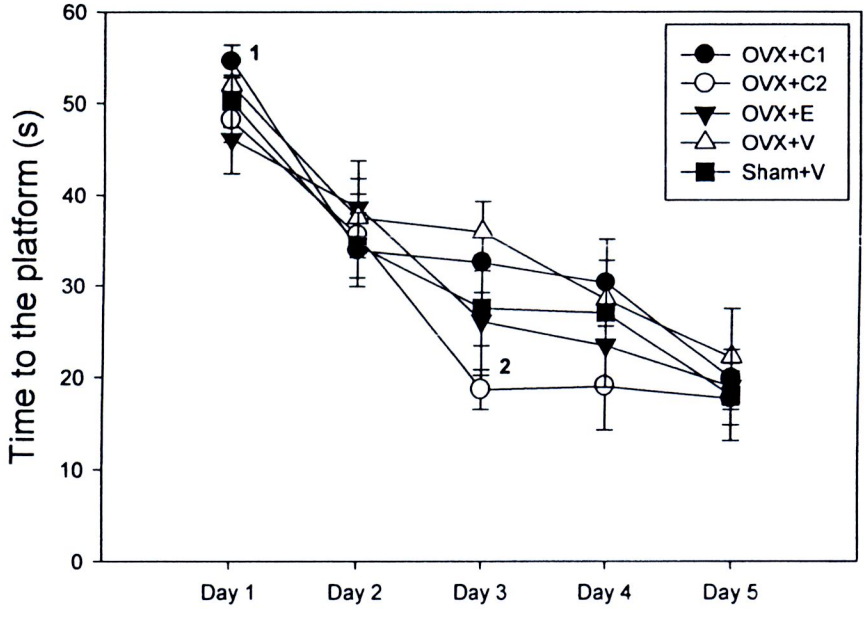

Figure 19 The time to the platform at the 1st period long-term hidden platform test.

1. denoted the significant difference from OVX+C1 to OVX+E group.
2. denoted the significant difference from OVX+C2 to OVX+C1 and OVX+V groups.

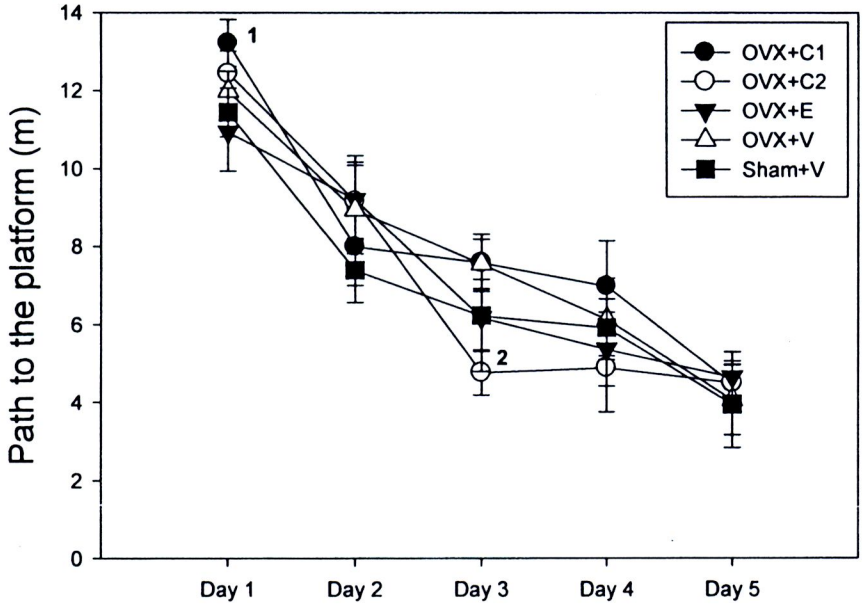

Figure 20 The path to the platform at the 1st period long-term hidden platform test.

1. denoted the significant difference from OVX+C1 to OVX+E group ($P<0.05$).
2. denoted the significant difference from OVX+C2 to OVX+C1 and OVX+V groups ($P<0.05$).

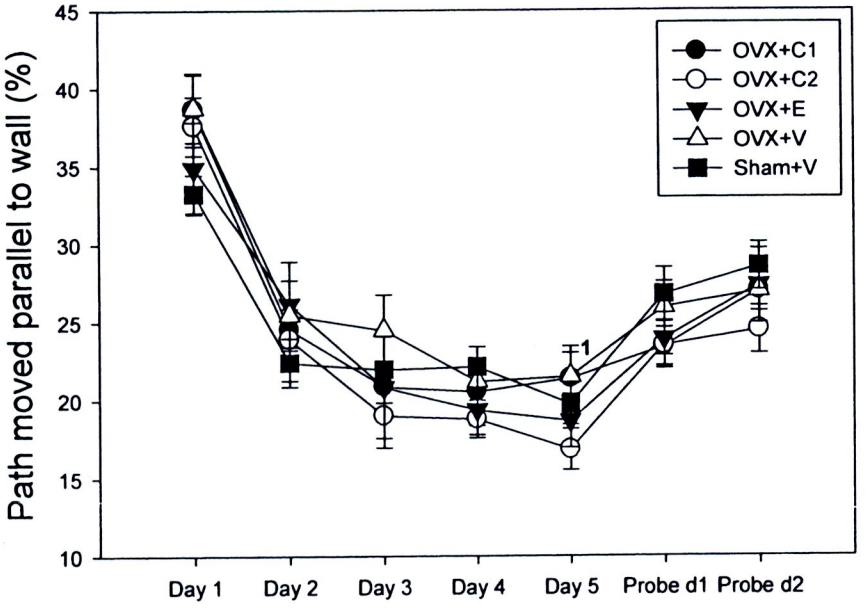

Figure 21 The path parallel to the wall at the 1st period long-term MWM test.

1. denoted the significant difference from OVX+V to OVX+C2 group ($P<0.05$).

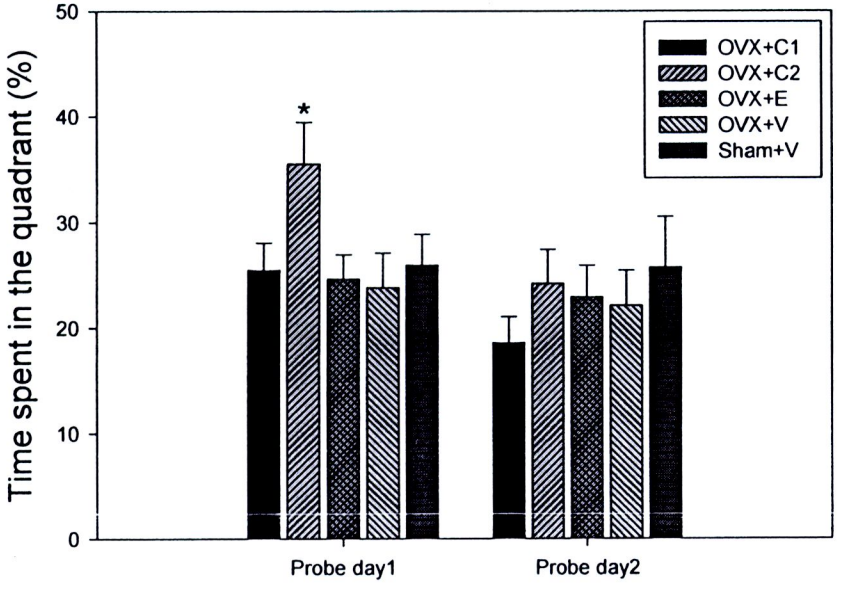

Figure 22 The time spent in the current goal quadrant (NE) at the 1st period long-term probe test.

* denoted the significant difference from OVX+C2 to the other 4 groups ($P<0.05$).

The motor ability related parameters of the animal, the swimming speed (m/s), active time (%), latency to move (s) and number of stops, were recorded and compared. OVX+C2 group had the highest swimming speed across the 1st period MWM test. OVX+C1, OVX+E, OVX+V and Sham+V groups had the similar swimming speed in the M-H1 test. In the probe test, the swimming speed increased in the OVX+E group but decreased in the OVX+C1 and Sham+V groups (Figure 23).

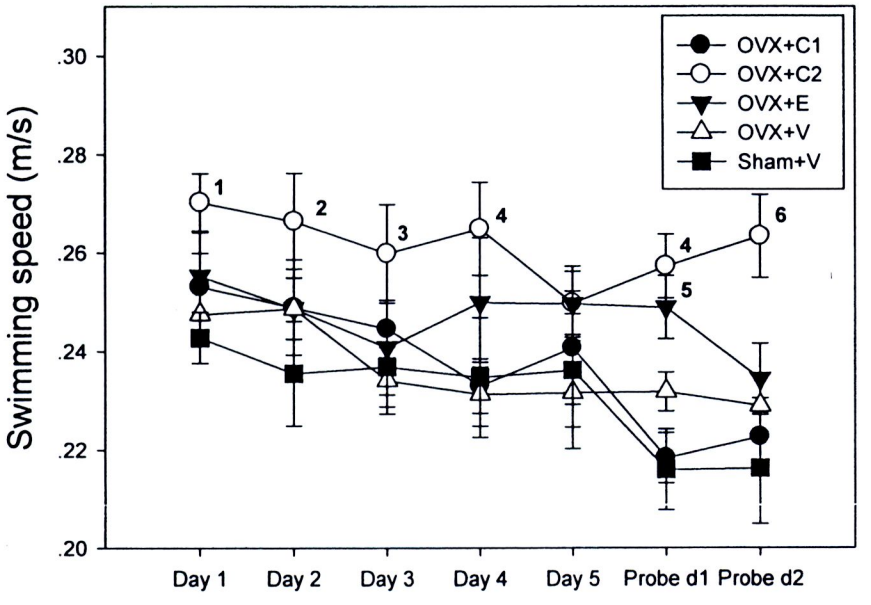

Figure 23 The swimming speed of the rats at the 1st period long-term MWM test.

1. denoted the significant difference from OVX+C2 to OVX+V and Sham+V groups ($P<0.05$).
2. denoted the significant difference from OVX+C2 to Sham+V group ($P<0.05$).
3. denoted the significant difference from OVX+C2 to OVX+V group ($P<0.05$).
4. denoted the significant difference from OVX+C2 to OVX+C1, OVX+V and Sham+V groups ($P<0.05$).
5. denoted the significant difference from OVX+E to OVX+C1 and Sham+V groups ($P<0.05$).
6. denoted the significant difference from OVX+C2 to the other 4 groups ($P<0.05$).

The OVX+C1, OVX+C2 and OVX+E groups had the similar and stable active time across the M-H1 test, while OVX+C1 had decreasing active time at the probe test. OVX+V and Sham+V groups had a gradually decreasing active time across the test and became the most non-active groups from the 3rd day of the test (Figure 24).

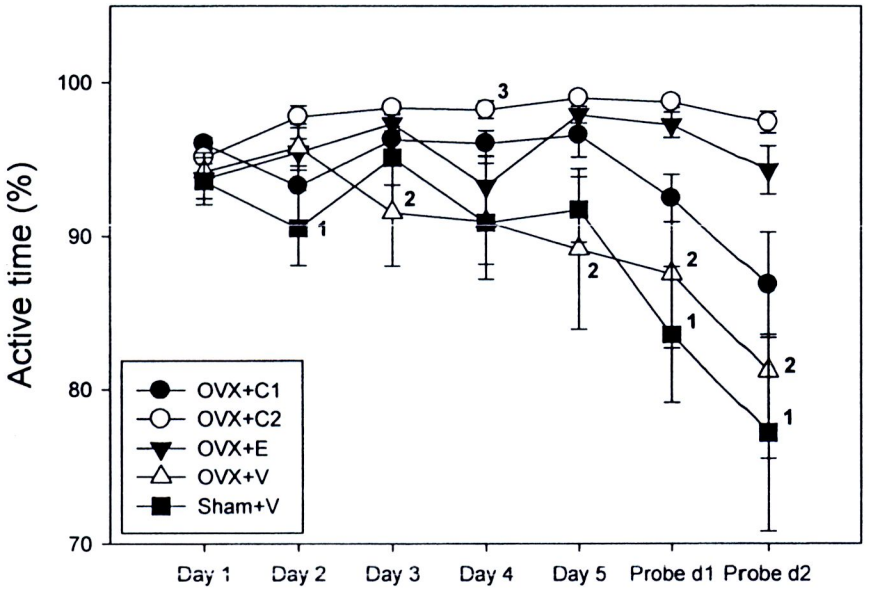

Figure 24 The active time of the rats at the 1st period long-term MWM test.

1. denoted the significant difference from Sham+V to OVX+C2 and OVX+V groups ($P<0.05$).
2. denoted the significant difference from OVX+V to OVX+C2 and OVX+E groups ($P<0.05$).
3. denoted the significant difference from OVX+C2 to OVX+V and Sham+V groups ($P<0.05$).

The OVX+C2 group had the lowest latency to move and number of stops; while the OVX+C1, OVX+V and Sham+V groups had higher latency to move and the number of stop, especially in the probe test (Figure 25-26).

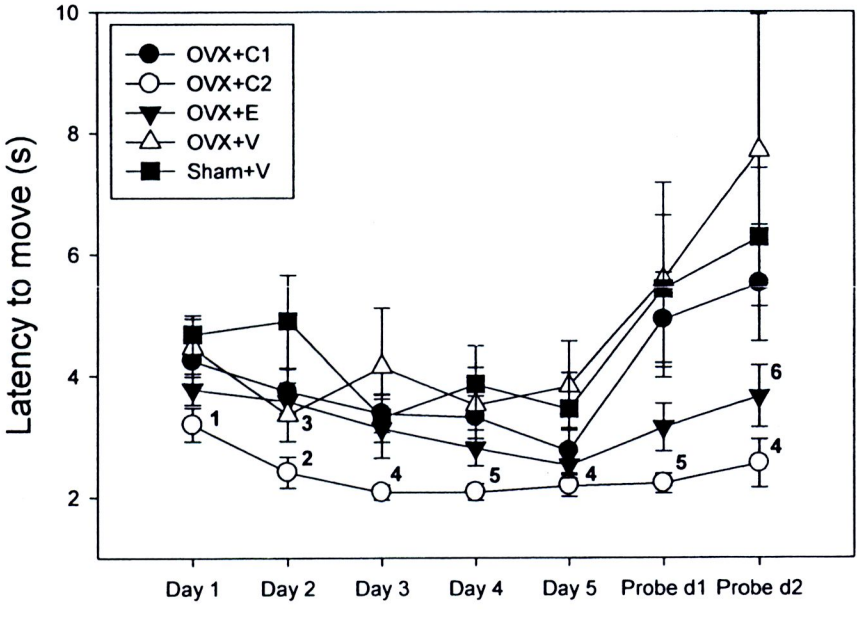

Figure 25 The latency of move of the rats at the 1st period long-term MWM test.

1. denoted the significant difference from OVX+C2 to OVX+C1, OVX+V and Sham+V groups ($P<0.05$).
2. denoted the significant difference from OVX+C2 to OVX+C1 and Sham+V groups ($P<0.05$).
3. denoted the significant difference from OVX+V to Sham+V group ($P<0.05$).
4. denoted the significant difference from OVX+C2 to OVX+V group ($P<0.05$).
5. denoted the significant difference from OVX+C2 to OVX+V and Sham+V groups ($P<0.05$).
6. denoted the significant difference from OVX+E to OVX+V group ($P<0.05$).

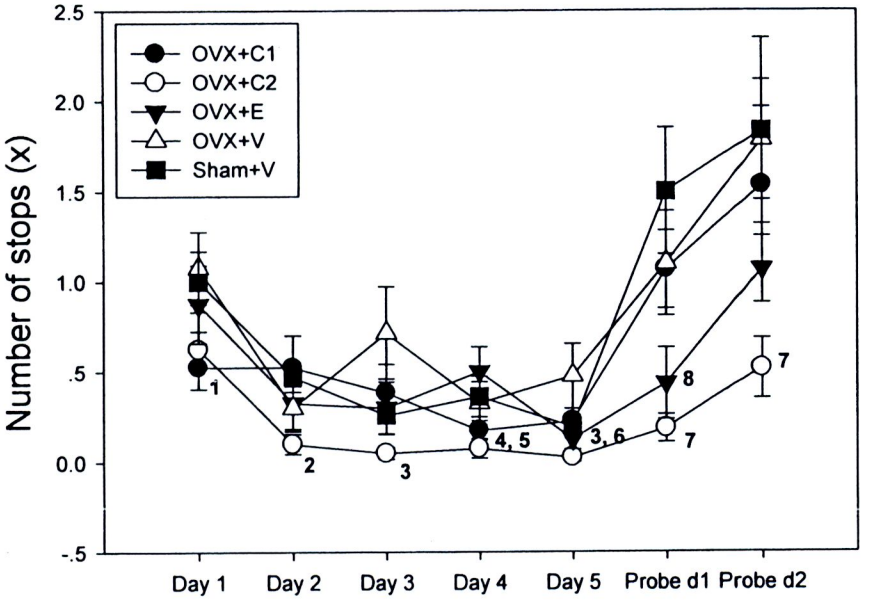

Figure 26 The number of stops of the rats at the 1st period long-term MWM test.

1. denoted the significant difference from OVX+C1 to OVX+V group ($P<0.05$).
2. denoted the significant difference from OVX+C2 to OVX+C1 and Sham+V groups ($P<0.05$).
3. denoted the significant difference from OVX+C2 to OVX+V group ($P<0.05$).
4. denoted the significant difference from OVX+C1 to OVX+E group ($P<0.05$).
5. denoted the significant difference from OVX+C2 to OVX+E group ($P<0.05$).
6. denoted the significant difference from OVX+E to OVX+V group ($P<0.05$).
7. denoted the significant difference from OVX+C2 to OVX+C1, OVX+V and Sham+V groups ($P<0.05$).
8. denoted the significant difference from OVX+E to Sham+V group ($P<0.05$).

b) The 2nd period

The OVX+V group used the longest time and path the reach the platform across the 5 days test at M-H2, indicating the memory impairment was happened. CHE and estradiol treatment on improved the performance of OVX+C1, OVX+C2 and OVX+E groups, which had the better performance in finding the hidden platform. Sham+V group had a better performance at the first and second day, but did not progress as much as the OVX+C1, OVX+C2 and OVX+E did at the last 3 days and reach the same level as OVX+V group at the end of the test (Figure 27-28). At the following probe test 30 days latter, OVX+V group spent the fewest time in the current goal quadrant, which was significantly less than the OVX+C2 group did at the 1st test day. The difference narrowed at the 2nd test day (Figure 29). The OVX+V had the longer path moved parallel to the wall across the test and joined by the Sham+V group from the 4th day (Figure 30).

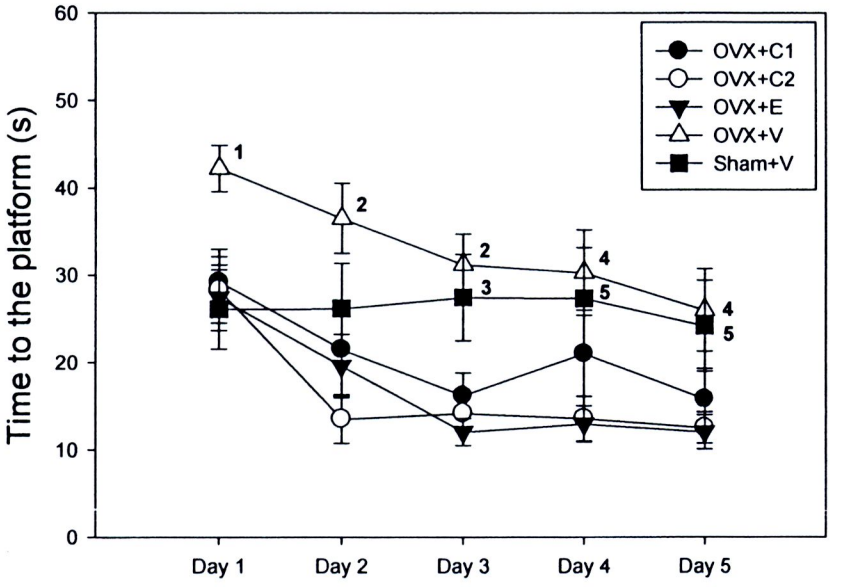

Figure 27 The time to the platform at the 2nd period long-term hidden platform test.

1. denoted the significant difference from OVX+V to the other 4 groups ($P<0.05$).
2. denoted the significant difference from OVX+V to OVX+C1, OVX+C2 and OVX+E groups ($P<0.05$).
3. denoted the significant difference from Sham+V to OVX+C1, OVX+C2 and OVX+E group ($P<0.05$)
4. denoted the significant difference from OVX+V to OVX+C2 and OVX+E group ($P<0.05$)
5. denoted the significant difference from Sham+V to OVX+C2 and OVX+E group ($P<0.05$)

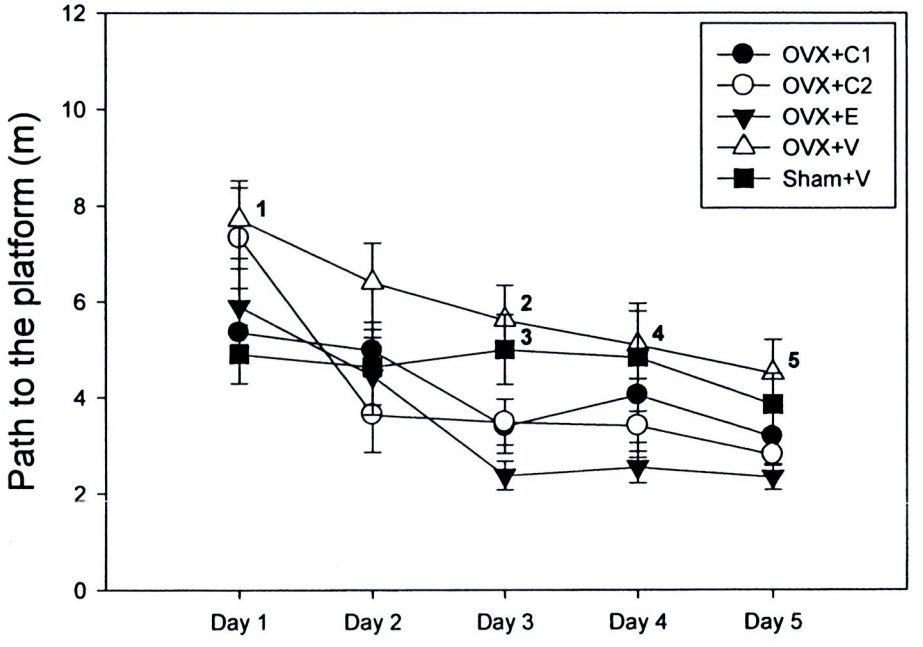

Figure 28 The path to the platform at the 2nd period long-term hidden platform test.

1. denoted the significant difference from OVX+V to OVX+C1 and Sham+V ($P<0.05$).
2. denoted the significant difference from OVX+V to OVX+C1, OVX+C2 and OVX+E groups ($P<0.05$).
3. denoted the significant difference from Sham+V to OVX+E group ($P<0.05$)
4. denoted the significant difference from OVX+V to OVX+E group ($P<0.05$)
5. denoted the significant difference from OVX+V to OVX+C2 and OVX+E groups ($P<0.05$)

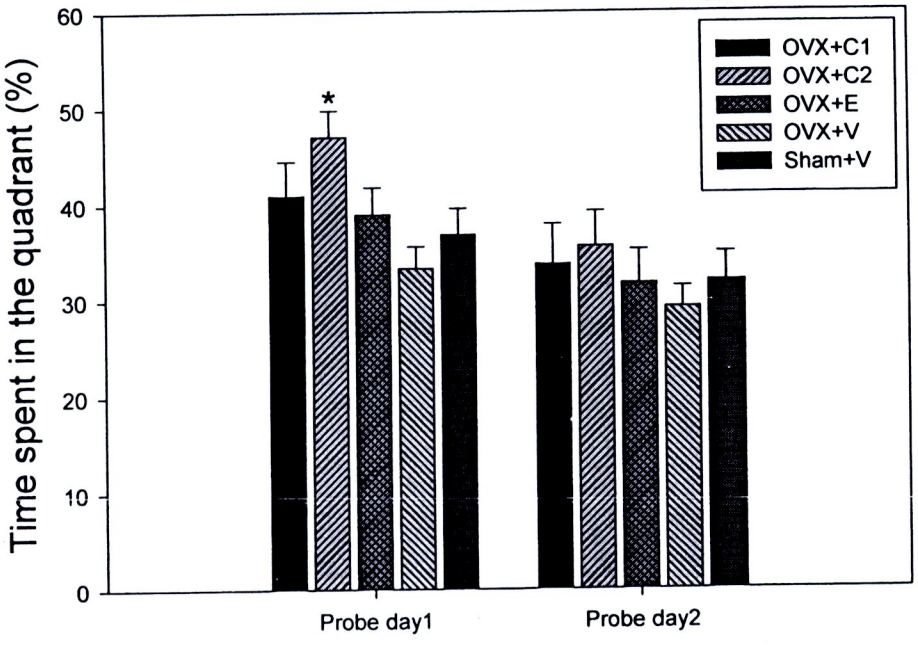

Figure 29 The time spent in the current goal quadrant at the 2nd period long-term probe test.

* significantly different to OVX+V and Sham+V groups ($P<0.05$).

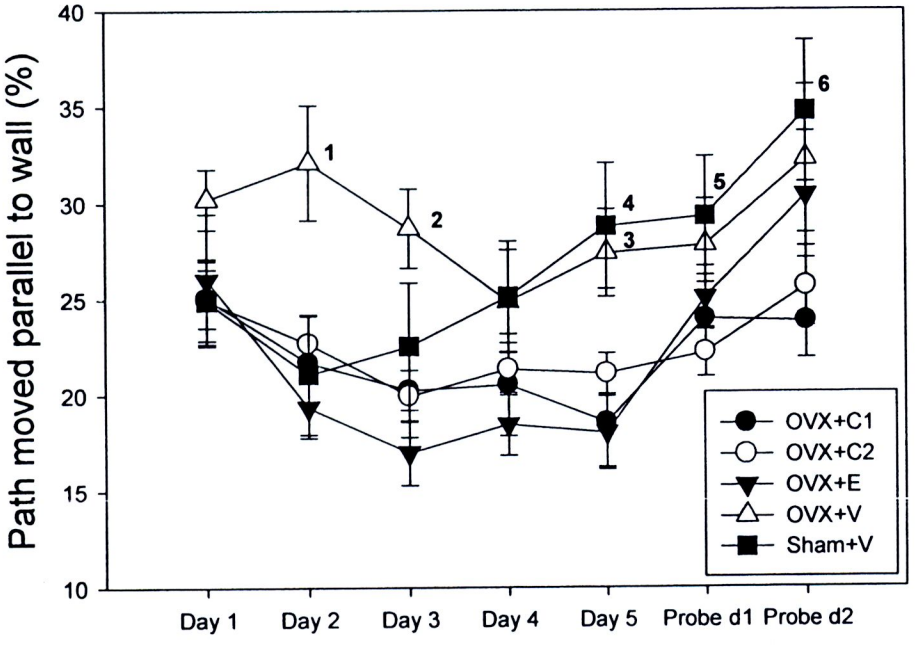

Figure 30 The path move parallel to the wall at the 2nd period MWM test.

1. denoted the significant difference from OVX+V to the other 4 groups ($P<0.05$).
2. denoted the significant difference from OVX+V to OVX+C1, OVX+C2 and OVX+E groups ($P<0.05$)
3. denoted the significant difference from OVX+V to OVX+C1 and OVX+E groups ($P<0.05$)
4. denoted the significant difference from Sham+V to OVX+C1, OVX+C2 and OVX+E groups ($P<0.05$)
5. denoted the significant difference from Sham+V to OVX+C2 group ($P<0.05$)
6. denoted the significant difference from Sham+V to OVX+C1 group ($P<0.05$)

The swimming speed (m/s), active time (%), latency to move (s) and number of stops of the animal at the 2nd MWM test period were recorded and show at the Figure 4.31-4.34.

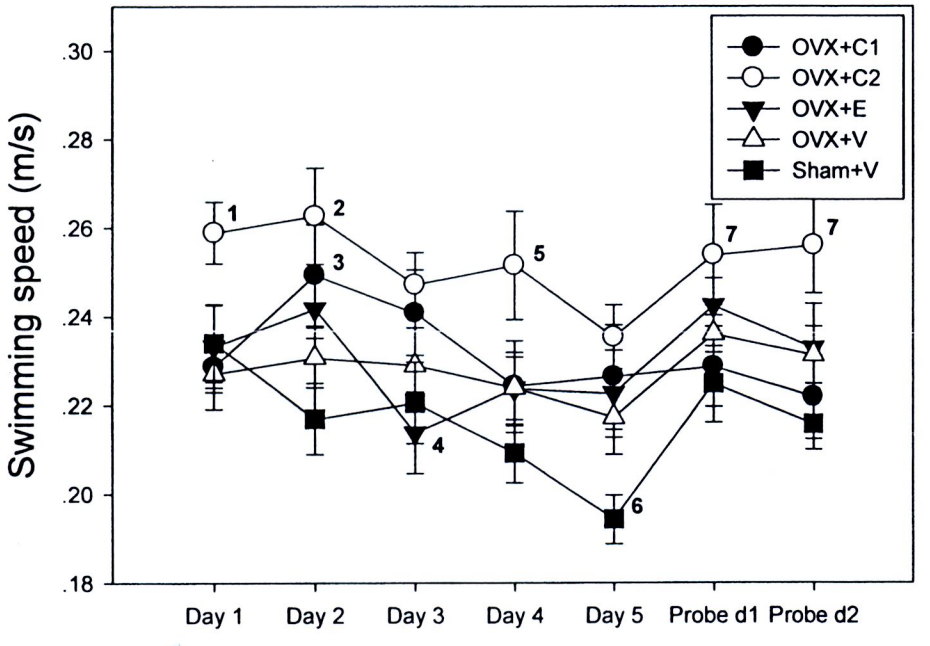

Figure 31 The swimming speed of the rats at the 2nd period of the MWM test

1. denoted the significant difference from OVX+E to OVX+C1, OVX+E and OVX+V groups ($P<0.05$)
2. denoted the significant difference from OVX+C2 to OVX+V and Sham+V groups ($P<0.05$)
3. denoted the significant difference from OVX+C1 to Sham+V group ($P<0.05$).
4. denoted the significant difference from OVX+E to OVX+C1 and OVX+C2 groups ($P<0.05$)
5. denoted the significant difference from OVX+C2 to Sham+V group ($P<0.05$)
6. denoted the significant difference from Sham+V to the OVX+C1 and OVX+C2 groups ($P<0.05$)
7. denoted the significant difference from OVX+C2 to OVX+C1 and Sham+V group ($P<0.05$)

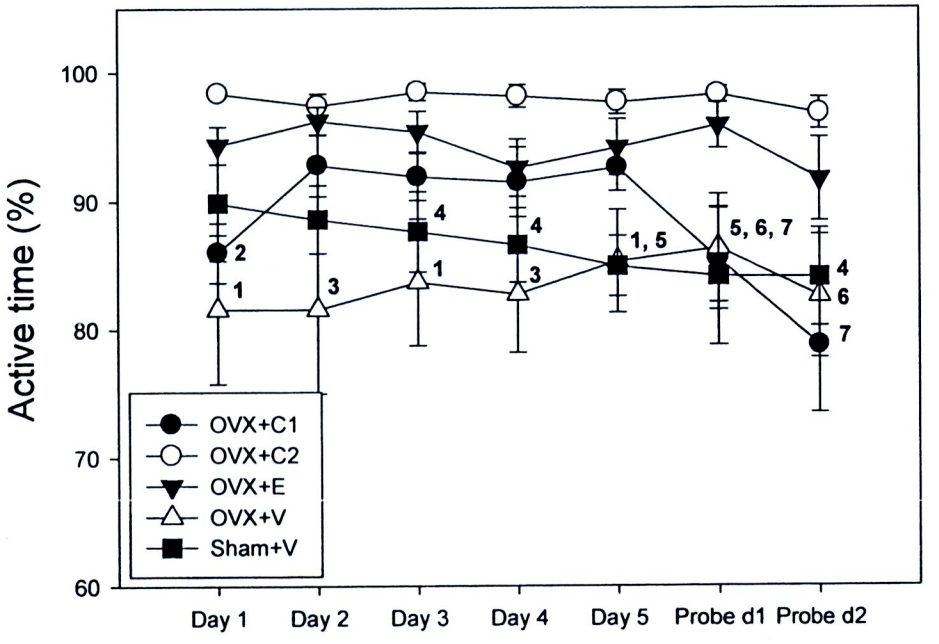

Figure 32 The active time of the rats at the 2nd period of the MWM test

1. denoted the significant difference from OVX+V to OVX+C2 and OVX+E groups ($P<0.05$)
2. denoted the significant difference from OVX+C1 to OVX+C2 group ($P<0.05$)
3. denoted the significant difference from OVX+V to OVX+C1, OVX+C2 and OVX+E groups ($P<0.05$).
4. denoted the significant difference from Sham+V to OVX+C2 groups ($P<0.05$)
5. denoted the significant difference from Sham+V to OVX+C2 and OVX+E groups ($P<0.05$)
6. denoted the significant difference from OVX+V to OVX+C2 groups ($P<0.05$)
7. denoted the significant difference from OVX+C1 to OVX+C2 group ($P<0.05$)

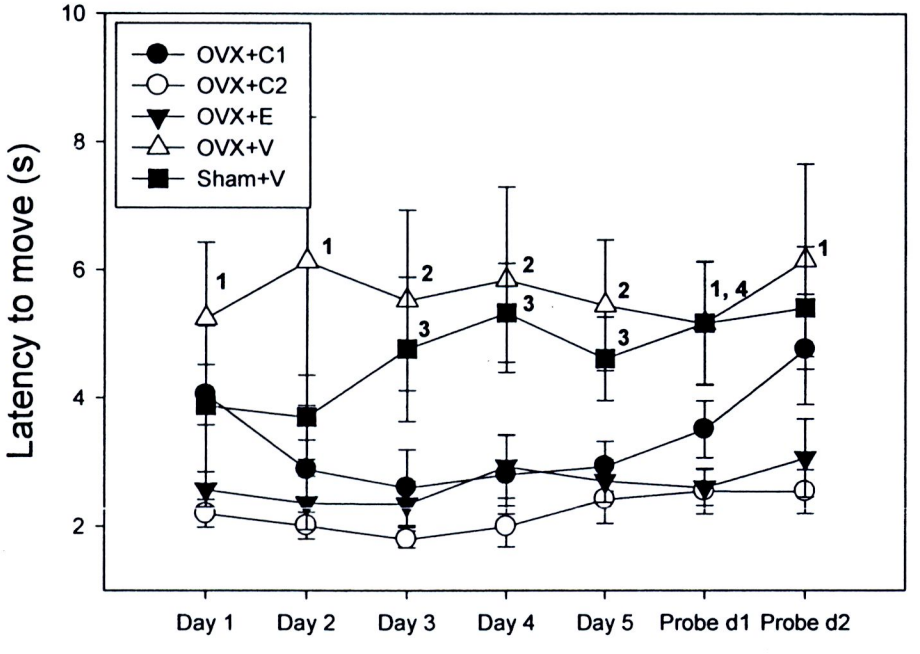

Figure 33 The latency to move of the rats at the 2nd period of the MWM test

1. denoted the significant difference from OVX+V to OVX+C2 and OVX+E groups ($P<0.05$)
2. denoted the significant difference from OVX+V to OVX+C1, OVX+C2 and OVX+E groups ($P<0.05$).
3. denoted the significant difference from Sham+V to OVX+C2 group ($P<0.05$)
4. denoted the significant difference from Sham+V to OVX+C2 and OVX+E groups ($P<0.05$)

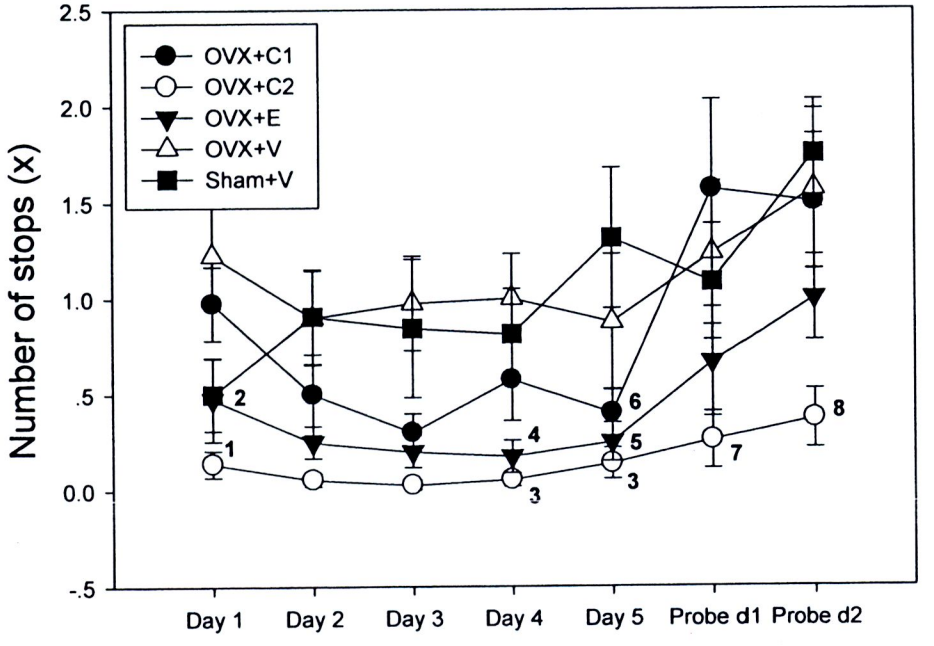

Figure 34 The number of stops of the rats at the 2nd period of the MWM test

1. denoted the significant difference from OVX+C2 to OVX+V group ($P<0.05$)
2. denoted the significant difference from OVX+E to OVX+V group ($P<0.05$)
3. denoted the significant difference from OVX+C2 to OVX+V and Sham+V groups ($P<0.05$).
4. denoted the significant difference from OVX+E to OVX+V and Sham+V groups ($P<0.05$)
5. denoted the significant difference from OVX+E to Sham+V groups ($P<0.05$)
6. denoted the significant difference from OVX+C1 to Sham+V groups ($P<0.05$)
7. denoted the significant difference from OVX+C2 to OVX+C1 and OVX+V group ($P<0.05$)
8. denoted the significant difference from OVX+C2 to OVX+C1, OVX+V and Sham+V groups ($P<0.05$)

c) *The 3rd period*

The OVX+V group still used the longer time and path to find the platform while the CHE and estradiol treatment improved the performance, but the difference between groups was narrowed when compared to the 2nd period (Figure 35-36). OVX+V group had the high percentage while OVX+C2 had the lower percentage of the path moved parallel to the wall, which indicated the path efficiency and the strategy to find the platform (Figure 37). At the following probe test, CHE and estradiol treated groups had the higher retention times spent in the current goal quadrant (Figure 38).

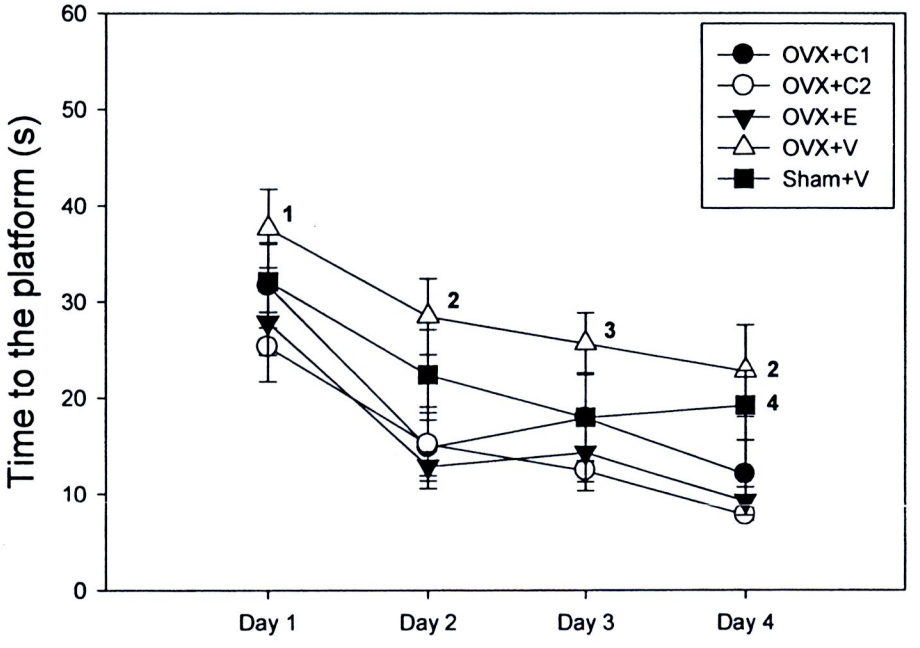

Figure 35 The time to the platform of the rats at the 3rd period of long-term hidden platform test.

1. denoted the significant difference from OVX+V to OVX+C2 group ($P<0.05$)
2. denoted the significant difference from OVX+V to OVX+C1, OVX+C2 and OVX+E group ($P<0.05$)
3. denoted the significant difference from OVX+V to OVX+C2 and OVX+E groups ($P<0.05$).
4. denoted the significant difference from Sham+V to OVX+C2 groups ($P<0.05$)

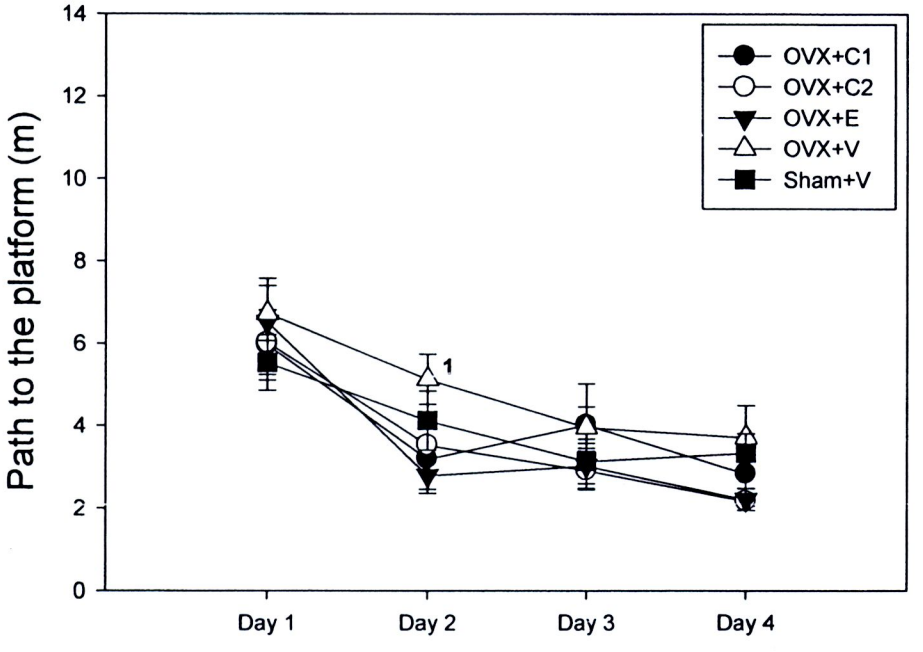

Figure 36 The path to the platform of the rats at the 3rd period of long-term hidden platform test.

1. denoted the significant difference from OVX+V to OVX+C1 and OVX+E group ($P<0.05$)

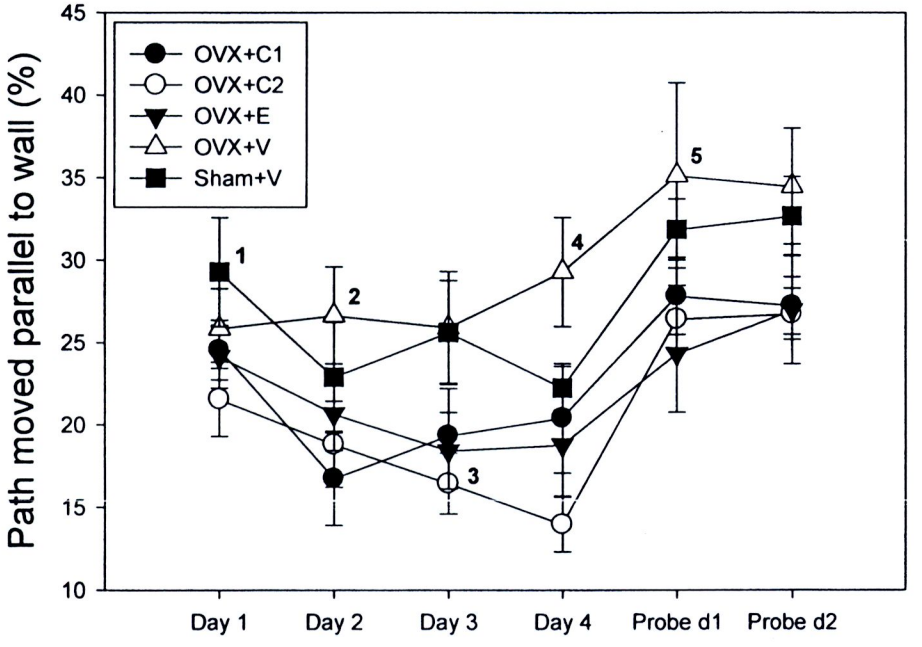

Figure 37 The path move parallel to the platform of the rats at the 3rd period of MWM test.

1. denoted the significant difference from Sham+V to OVX+C2 group ($P<0.05$)
2. denoted the significant difference from OVX+V to OVX+C1 group ($P<0.05$)
3. denoted the significant difference from OVX+C2 to OVX+V and Sham+V group ($P<0.05$)
4. denoted the significant difference from OVX+V to OVX+C1, OVX+C2 and OVX+E group ($P<0.05$)
5. denoted the significant difference from OVX+V to OVX+E group ($P<0.05$)

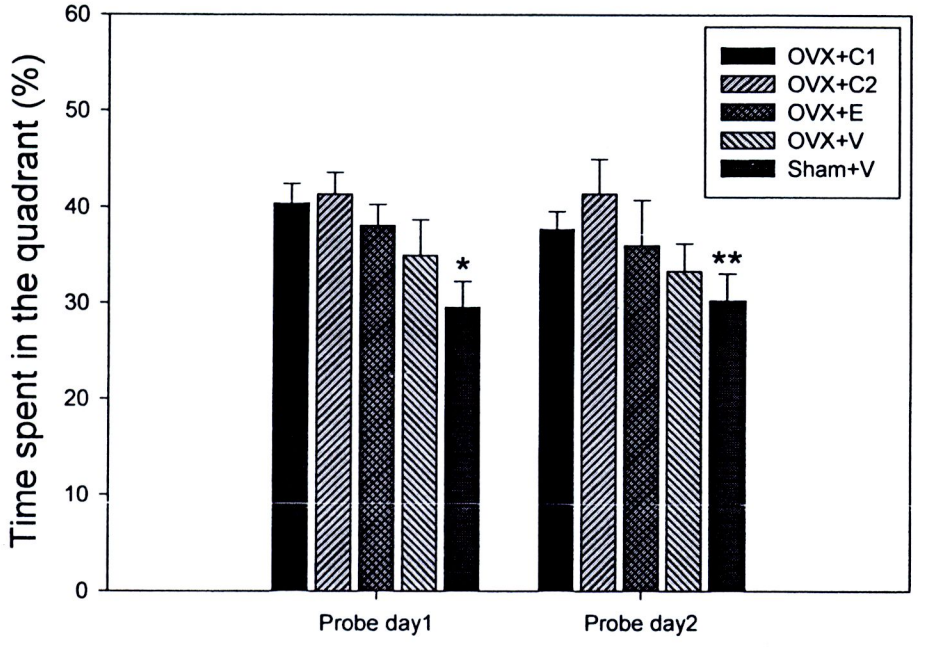

Figure 38 The path move parallel to the platform of the rats at the 3rd period of MWM test.

*. significantly different to OVX+C1, OVX+C2 and OVX+E groups ($P<0.05$)

**. significantly different to OVX+C2 group ($P<0.05$)

The swimming speed (m/s), active time (%), latency to move (s) and number of stops were recorded and showed as Figure 39-42

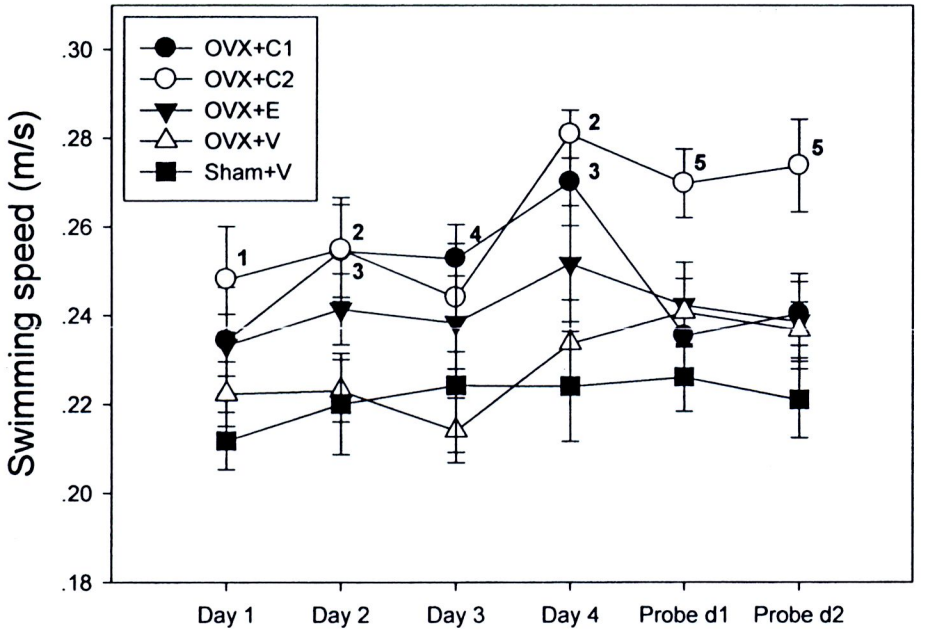

Figure 39 The swimming speed of the rats at the 3rd period of long-term MWM test.

1. denoted the significant difference from OVX+C2 to Sham+V group ($P<0.05$)
2. denoted the significant difference from OVX+C2 to OVX+V and Sham+V groups ($P<0.05$)
3. denoted the significant difference from OVX+C1 to OVX+V and Sham+V groups ($P<0.05$)
4. denoted the significant difference from OVX+C1 to OVX+V group ($P<0.05$)
5. denoted the significant difference from OVX+C2 to the other 4 groups ($P<0.05$)

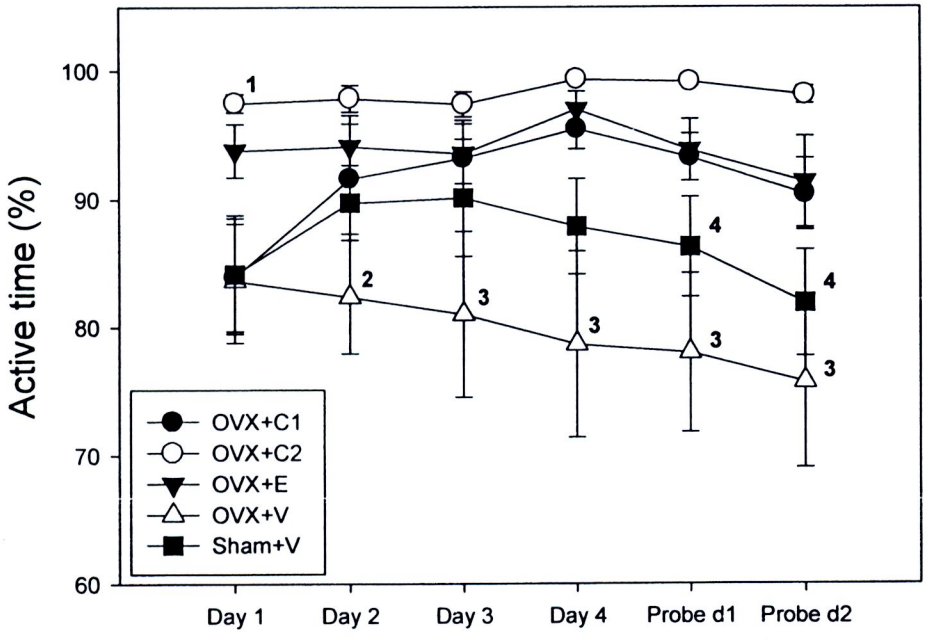

Figure 40 The active time of the rats at the 3rd period of long-term MWM test.

1. denoted the significant difference from OVX+C2 to OVX+C1, OVX+V and Sham+V group ($P<0.05$)
2. denoted the significant difference from OVX+V to OVX+C2 and OVX+E groups ($P<0.05$)
3. denoted the significant difference from OVX+V to OVX+C1, OVX+C2 and OVX+E groups ($P<0.05$)
4. denoted the significant difference from Sham+V to OVX+C2 group ($P<0.05$)

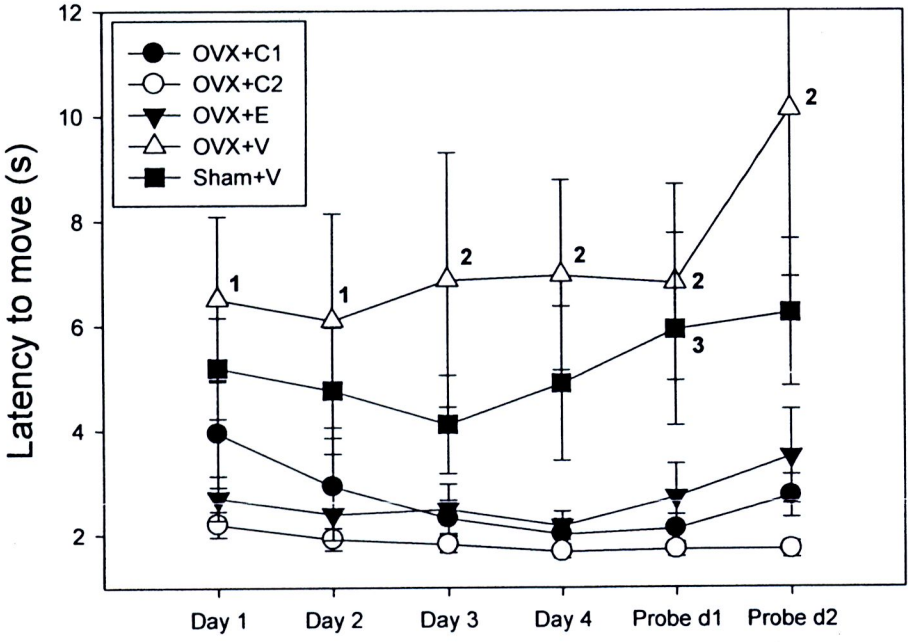

Figure 41 The latency to move of the rats at the 3rd period of long-term MWM test.

1. denoted the significant difference from OVX+V to OVX+C2 and OVX+E groups ($P<0.05$)
2. denoted the significant difference from OVX+V to OVX+C1, OVX+C2 and OVX+E groups ($P<0.05$)
3. denoted the significant difference from Sham+V to OVX+C1 and OVX+C2 groups ($P<0.05$)

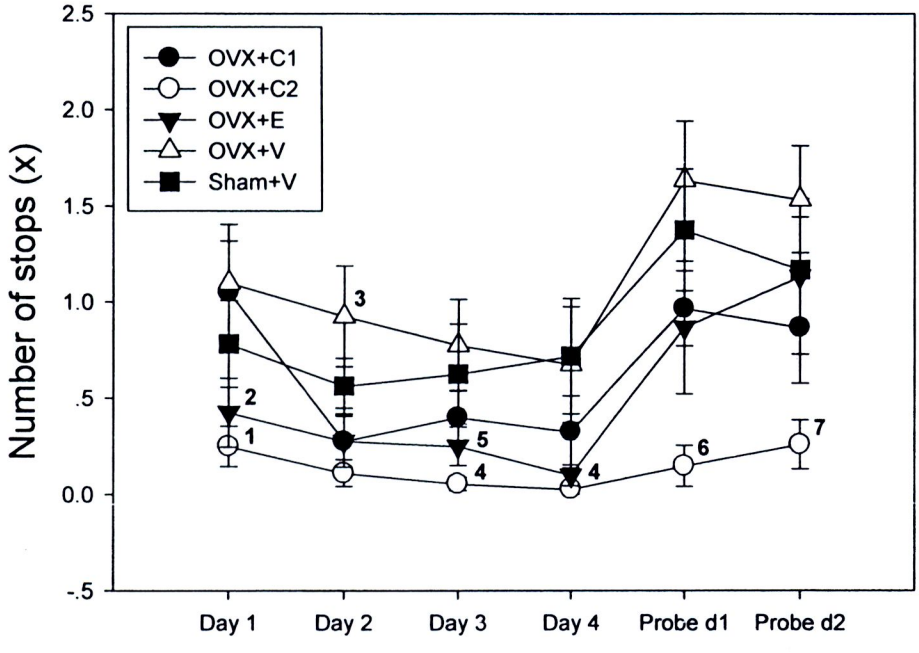

Figure 42 The number of stops of the rats at the 3rd period of long-term MWM test.

1. denoted the significant difference from OVX+C2 to OVX+C1 and OVX+V groups ($P<0.05$)
2. denoted the significant difference from OVX+E to OVX+C1 and OVX+V groups ($P<0.05$)
3. denoted the significant difference from OVX+V to OVX+C1, OVX+C2 and OVX+E groups ($P<0.05$)
4. denoted the significant difference from OVX+C2 to OVX+V and Sham+V groups ($P<0.05$)
5. denoted the significant difference from OVX+E to OVX+V group ($P<0.05$)
6. denoted the significant difference from OVX+C2 to OVX+C1, OVX+V and Sham+V groups ($P<0.05$)
7. denoted the significant difference from OVX+C2 to OVX+E, OVX+V and Sham+V groups ($P<0.05$)

When comparing the learning ability of each groups between 3 periods, the progress of the OVX+C1, OVX+C2 and OVX+E groups were observed between the 1st and 2nd period, with little difference from the 2nd to the 3rd period. (Figure 43, A, B, C). It was noticed that the Sham+V group, which had no progress across the 2nd period, even though they were faster than the OVX+V group at the 1st day and 2nd day (Figure 43, E).

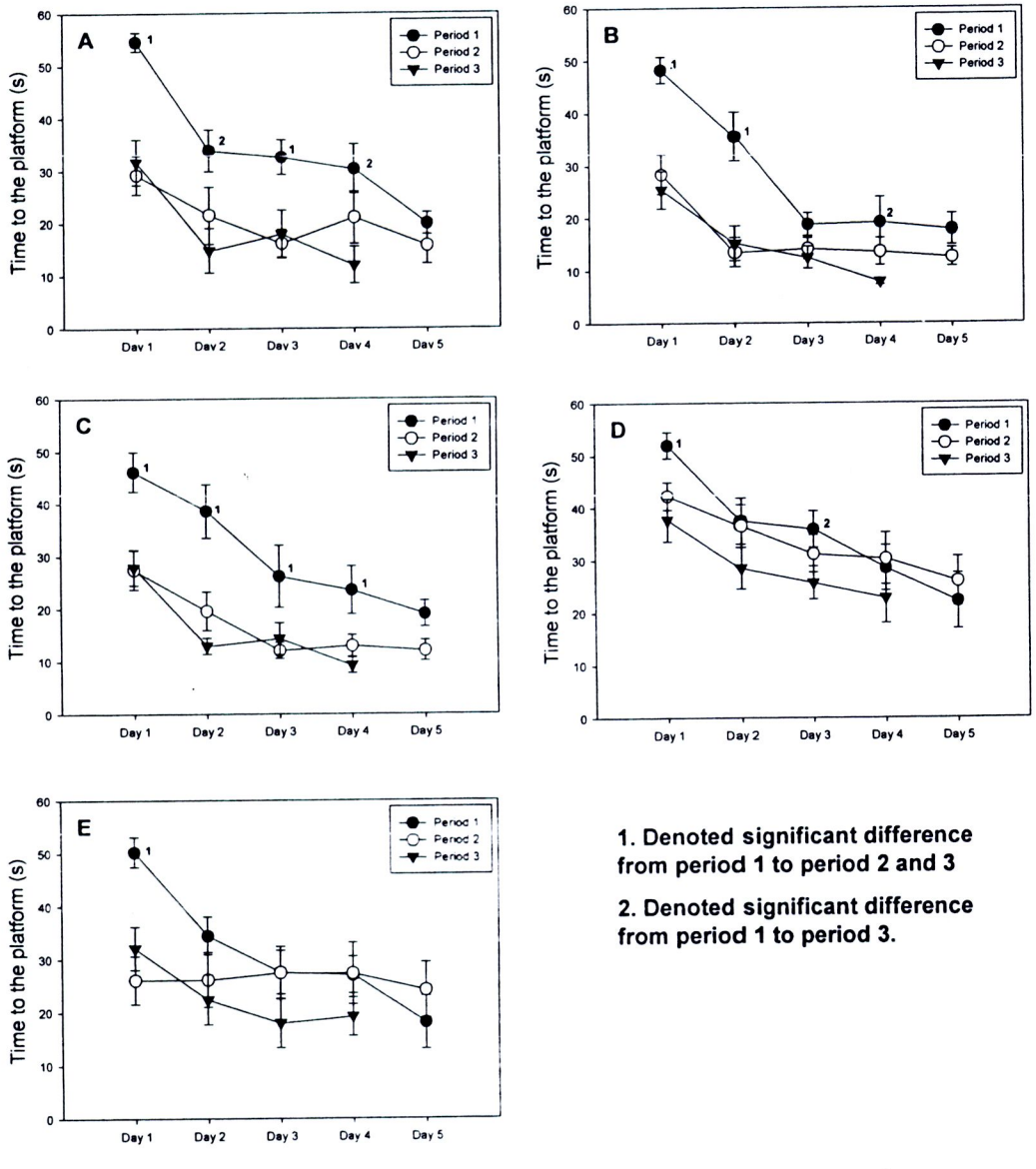

Figure 43 The comparison of the time to the platform from 1st to 3rd period of each group. A: OVX+C1; B: OVX+C2; C: OVX+E; D: OVX+V; E: Sham+V.

4.3.2 RAM test

Ovariectomy did not impair the spatial working memory at both the free accessible test and the delay non-match to sample (DNMTS) test of the present 8-arms radial arm maze test.

Different doses of CHE affected the performance at different periods. The OVX+C1 group made the smallest error at the free accessible test, but the delay time increased for the DNMTS test, with error times increasing the most out of the 5 groups. The reversed result was observed on the OVX+C2 group, which made the biggest error at the free accessible test and the smallest error at 2 hours DNMTS test. The OVX+E group and Sham+V performed equally for every test (Figure 44).

The data of the free accessible test and 1 hour DNMTS test at the 1st and 2nd period did not show a difference, indicating the OVX and the designed treatment did not affect the RAM performance on all 5 groups. (Figure 44, A, C)

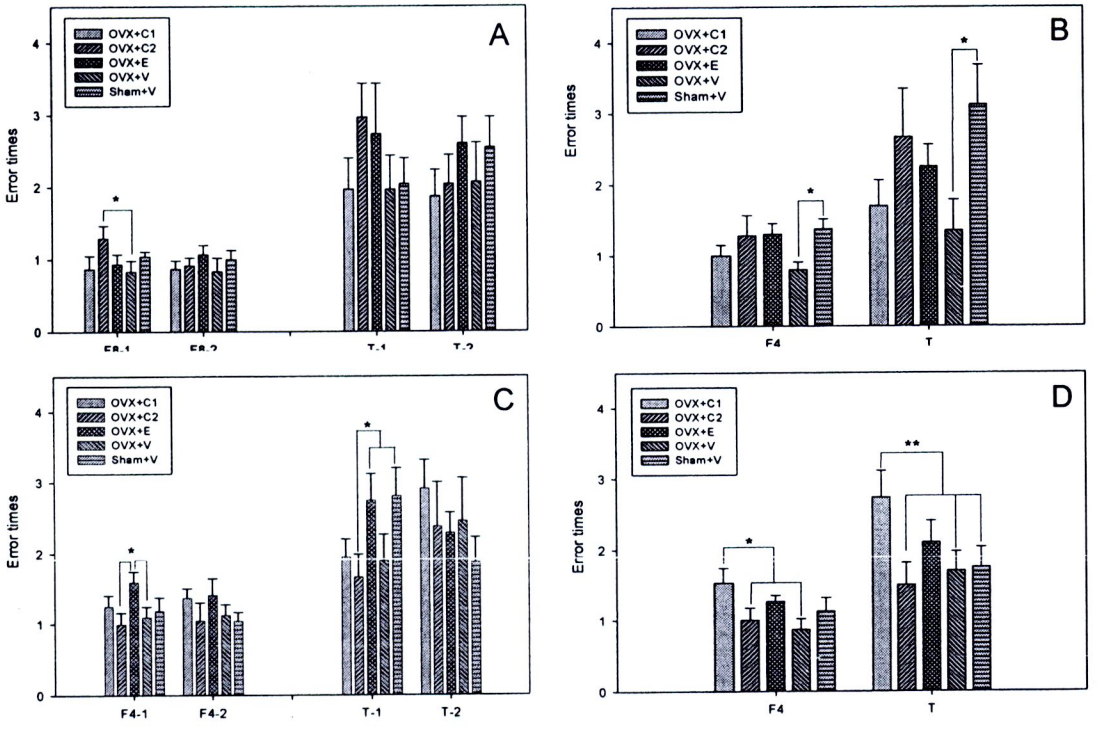

Figure 44 The error times (mean±SEM) at free accessible test (A), 10 minutes delay (B), 1 hour delay (C) and 2 hours delay (D) DNMTS test. F8 and F4 denoted the errors at the first 8 probes and first 4 probes at the free accessible and DNMTS tests respectively. T denoted the total error at probing the non-visit arms. The number -1 or -2 denoted the period 1 and period 2.

* Denoted the significant difference between groups ($P<0.05$).

4.3.3 The body weight and the uterus weight

The body weight of the OVX plus vehicle group surged after the rat recovered from the surgery (Figure 45). At the postmortem check, a significant decrease in uterus weight was observed (Figure 46), indicating evidence of OVX and estradiol efficiency.

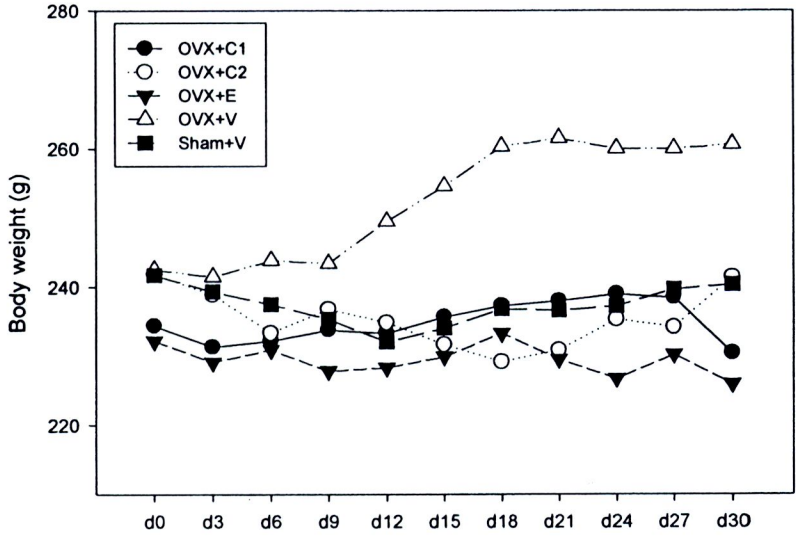

Figure 45 The body weight (Mean) of each group from day0 to day 30 after OVX. The body weight of OVX+V group surged and deviated from the other groups.

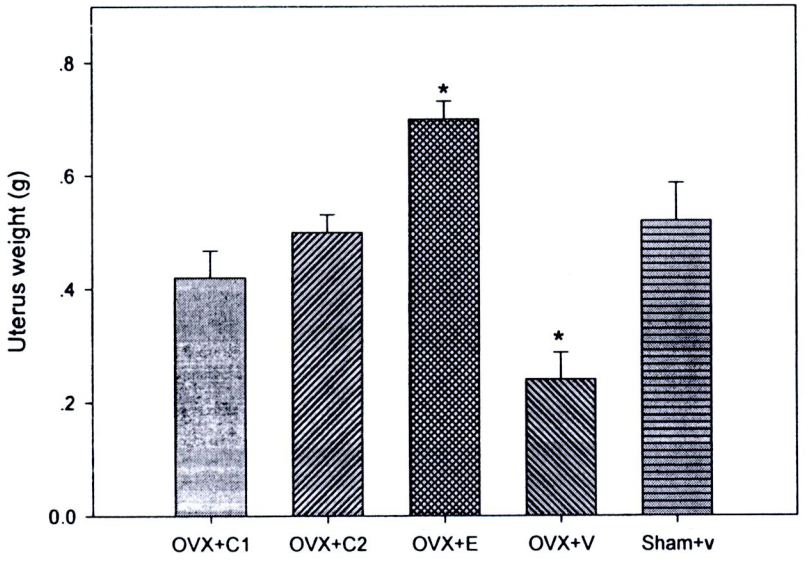

Figure 46 The uterus weight (mean±SEM) of each group in the long term behavior test

* Significantly different to the other 4 groups. ($p<0.05$)

4.4 Brain morphological study

4.4.1 Staining results

The brain section of AChE staining and Nissl staining were showed at Figure 47.

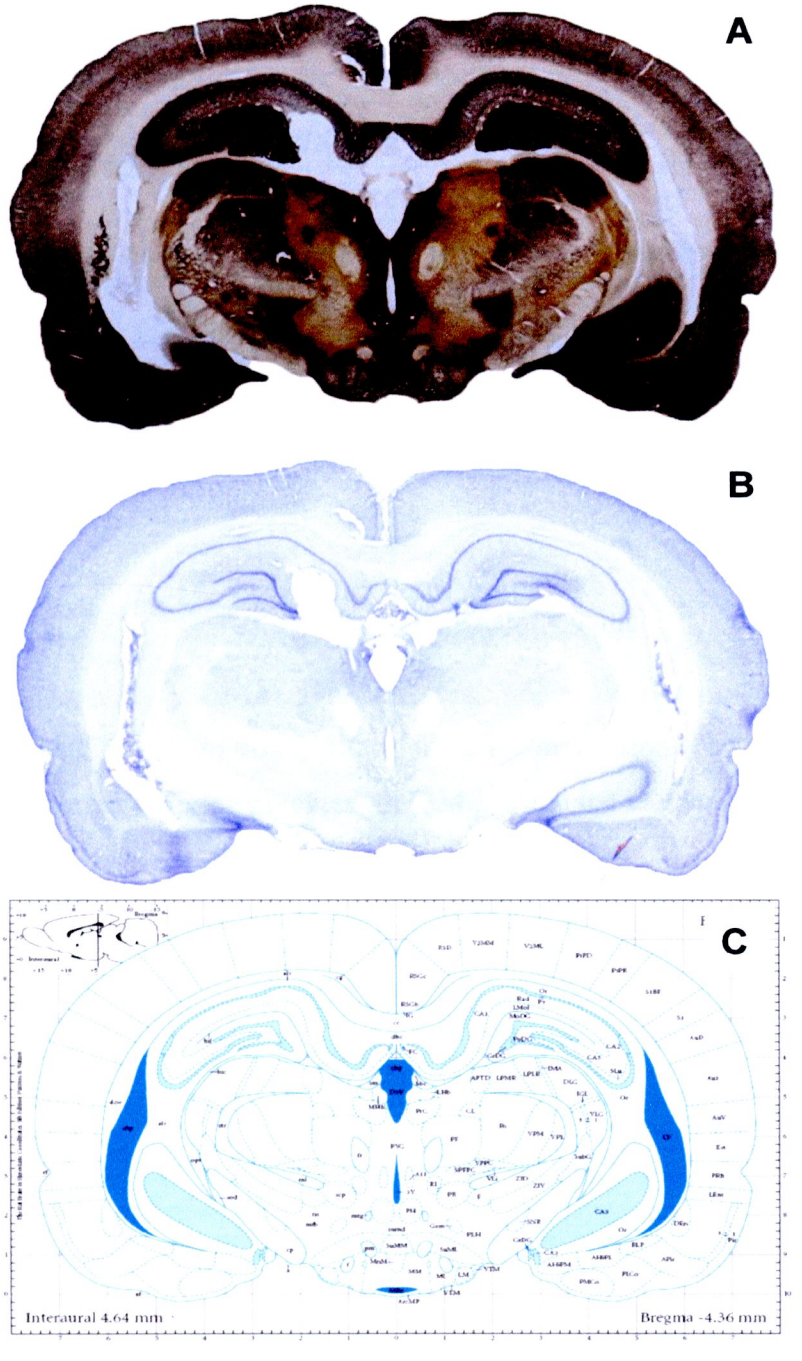

Figure 47 The AChE staining (A) and Nissl staining (B) results and the brain atlas (C) for identifying the segment of the specific region.

4.4.2 3D reconstruction of the rat brain and some of the functional areas.

a) Calibration

The *Measure Tool* of the 3D-Doctor was used to measure the pixel length of 10 millimeter which was taken from the same camera at the same optical condition while taking the photos of the rat brains (Figure 48). So the voxel width was calibrated as follows:

$$voxel\ width = \frac{length(real)}{length(pixel)} = \frac{10mm}{734.19} = 0.01362mm$$

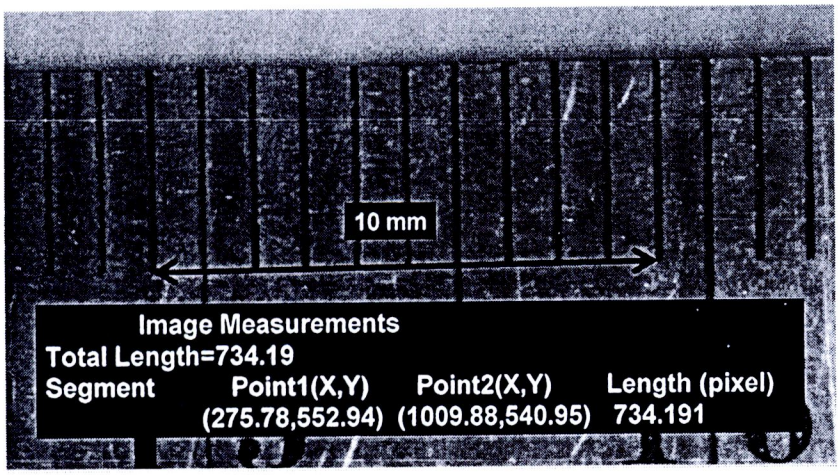

Figure 48 The calibration of voxel width for 3D reconstruction. The voxel width was calculated from the pixel length (734.19) and the real length (10 mm)

The intervals *between* the sections, 0.12 mm, which was calculated as Figure 49.

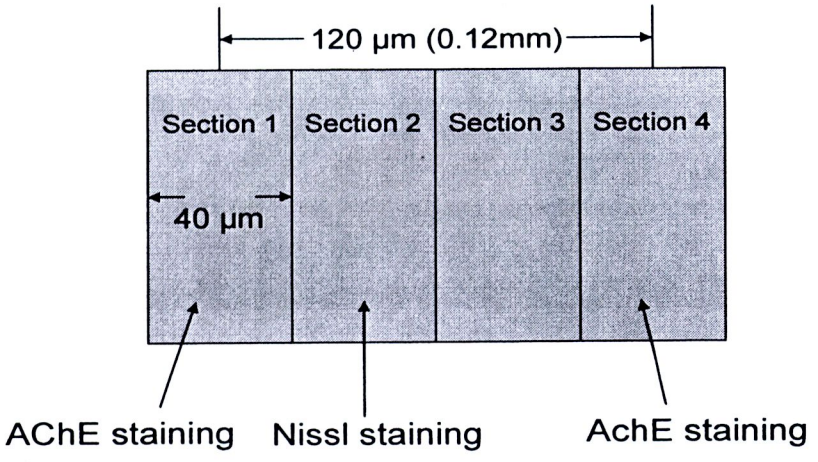

Figure 49 The calculation of the thickness between sections for 3D reconstruction. The 1st section of every three was used for AChE staining, the 2nd one was used for Nissl staining. The interval between AChE staining sections was 120 um.

b) 3D reconstruction of the brain structure

In the AChE staining sections, the cerebra, hippocampus, cortex, anterior commissure, caudate putamen, thalamus and basolateral amygdala were identified and segmented according to the rat brain atlas (Paxinos, 2004), followed by a reconstruction in 3 dimensions in the software (3D-Doctor) to construct a 3D model of these internal brain structures. The reconstructed 3D model could be observed from any positions to inspect their shapes and the related locations in the brain and to each others, providing a more intuitionistic vision than a traditional 2 dimensional images. Volume calculation was also available for measuring any reconstructed structures, which could tell directly the morphology changes in the structure and size. The ventral, anterior, lateral positions of the brain were provided in this report (Figure 50-57).

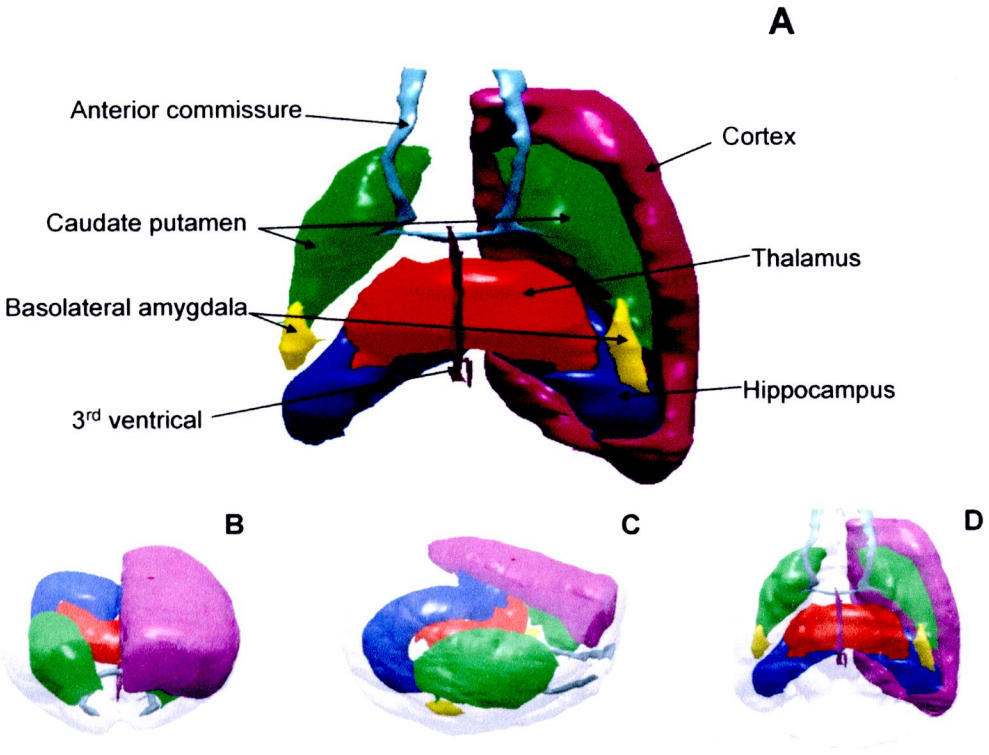

Figure 50 The location of the 3D reconstructed cerebra, anterior commissure, cortex, caudate putamen, basolateral amygdale, 3rd vertical, thalamus and hippocampus in the ventral position (A). Various vision angles were provided as B, C and D.

Basolateral amygdaloid (1.05 mm^3)

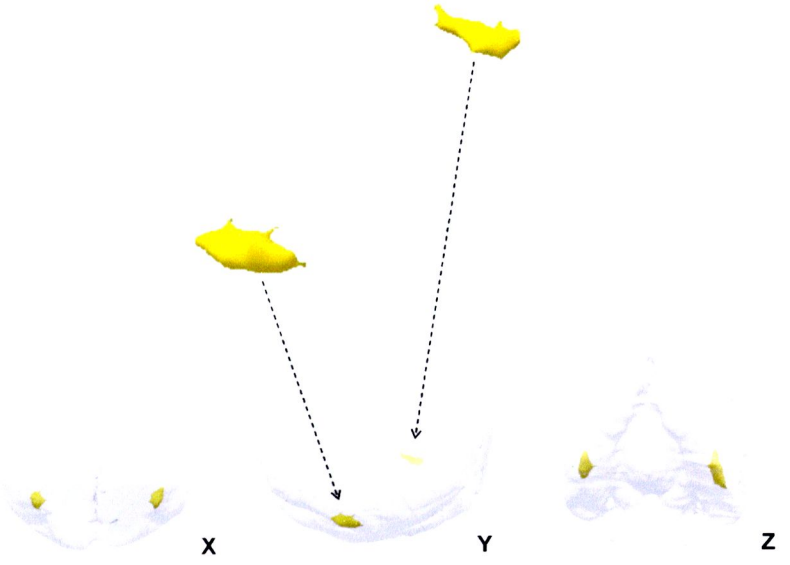

Figure 51 The shape and volume of the reconstructed basolateral amygdaloid and its location in the brain. Anterior (X), lateral (Y) and ventral (Z) visions of its location were provided.

Anterior commissure (1.05 mm^3)

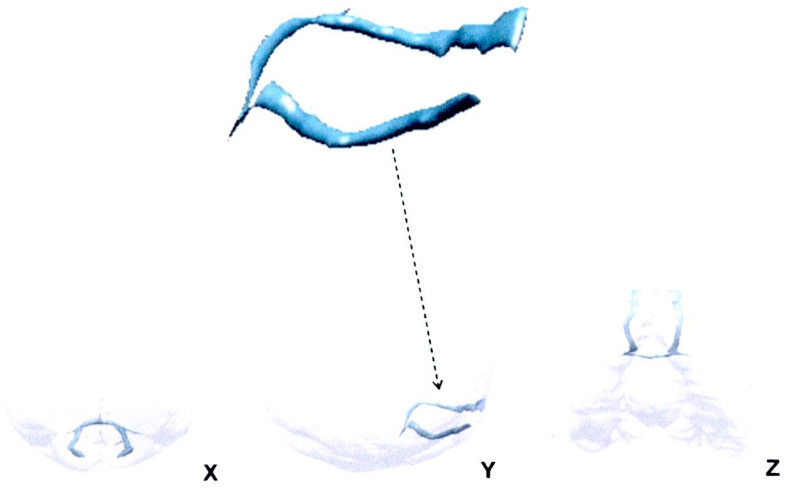

Figure 52 The shape and volume of a reconstructed anterior commissure and its location in the brain. Anterior (X), lateral (Y) and ventral (Z) visions of its location were provided.

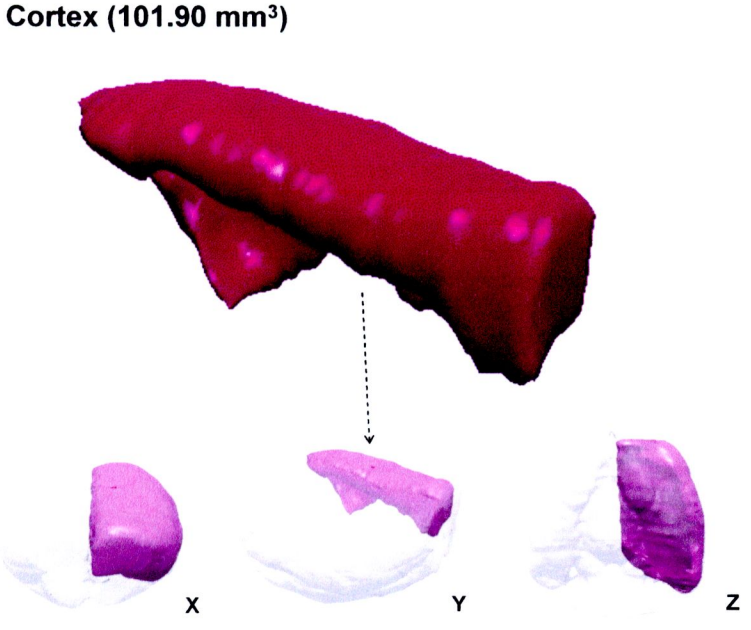

Figure 53 The shape and volume of a reconstructed cortex (left half) and its location in the brain. Anterior (X), lateral (Y) and ventral (Z) visions of its location were provided.

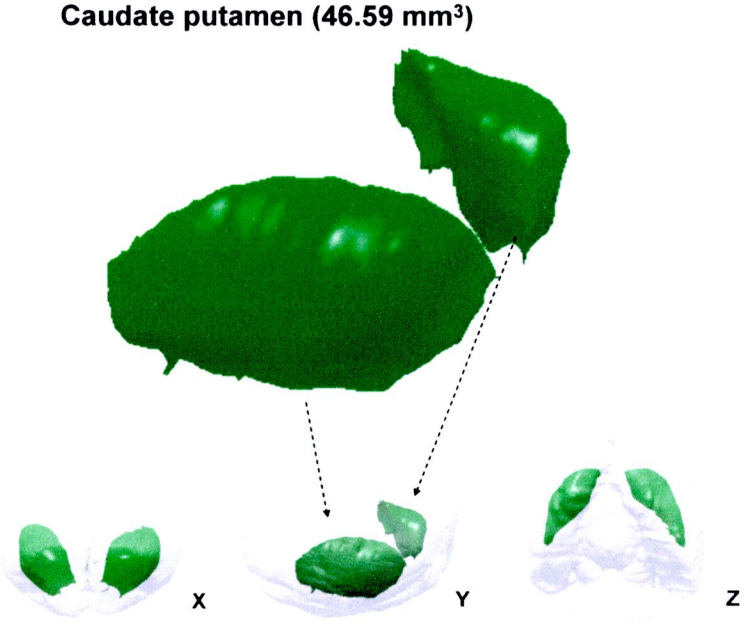

Figure 54 The shape and volume of the reconstructed caudate putamen and its location in the brain. Anterior (X), lateral (Y) and ventral (Z) visions of its location were provided.

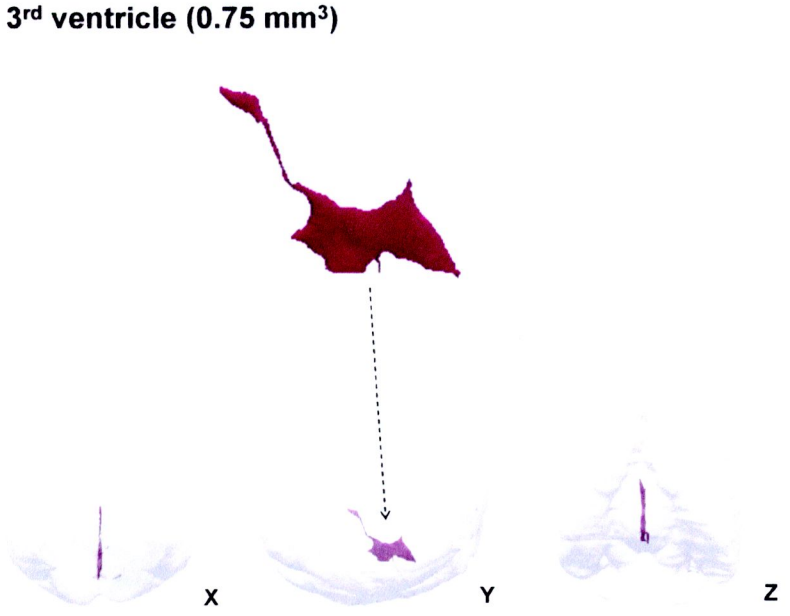

Figure 55 The shape and volume of a reconstructed 3rd ventricle and its location in the brain. Anterior (X), lateral (Y) and ventral (Z) visions of its location were provided.

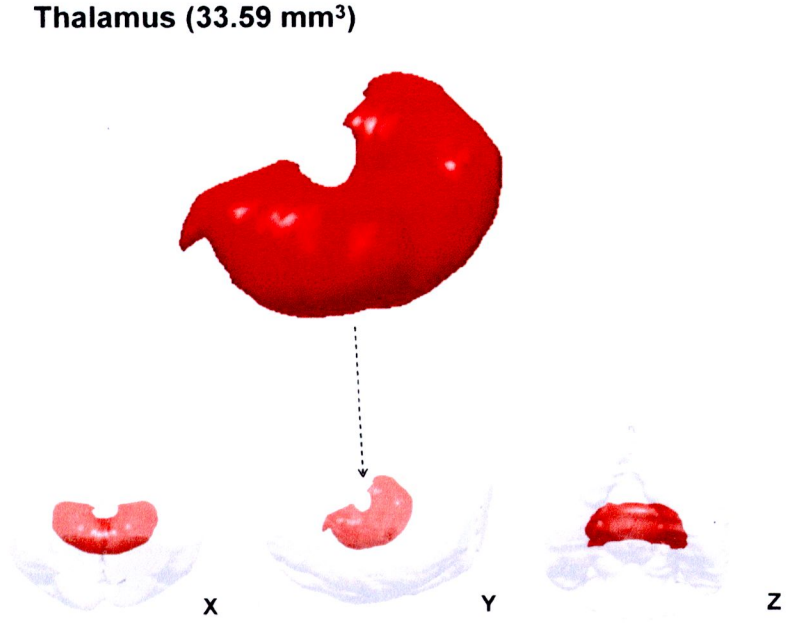

Figure 56 The shape and volume of a reconstructed thalamus and its location in the brain. Anterior (X), lateral (Y) and ventral (Z) visions of its location were provided.

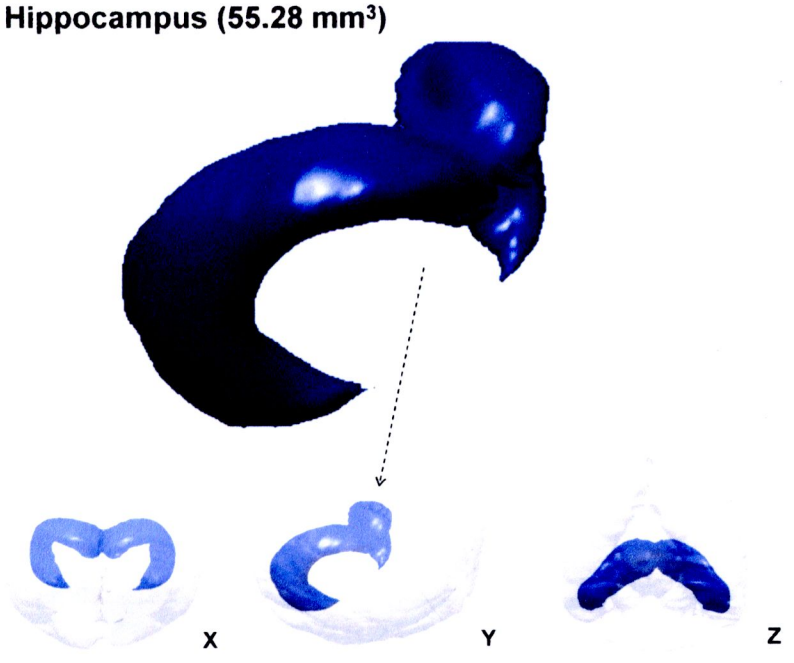

Figure 57 The shape and volume of a reconstructed hippocampus and its location in the brain. Anterior (X), lateral (Y) and ventral (Z) visions of its location were provided.

c) Volume of hippocampus

The hippocampal volume of each rat brain was calculated and compared between groups to evaluate the effect of the treatment (Figure 58). The body weight of each group was also compared. Of the absolute volume of hippocampus, the OVX+V group was the highest, followed by the Sham+V, OVX+E, OVX+C1 and OVX+C2 group, which was similar to the body weight of each group (Figure 59). The hippocampal volume per body weight (proportional hippocampus volume, mm^3/g) was also compared between groups. The OVX+C2 and OVX+E groups had the significant larger proportional hippocamal volume when compared to the OVX+V, OVX+C1 and Sham+V group (Figure 60)

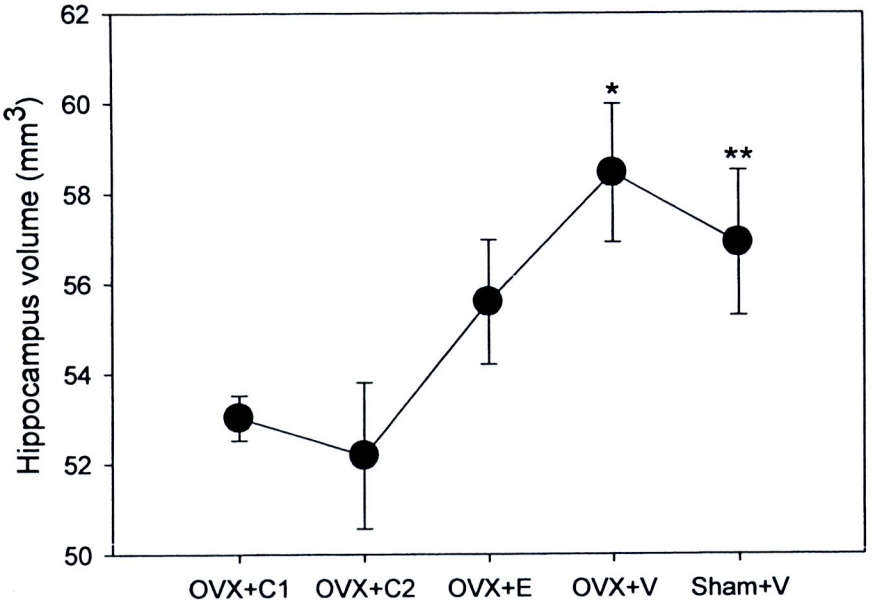

Figure 58 The hippocampal volume (mean±SEM) of each group.

* Significantly different to OVX+C1 and OVX+C2 ($p<0.05$).

** Significantly different to OVX+C2 ($p<0.05$).

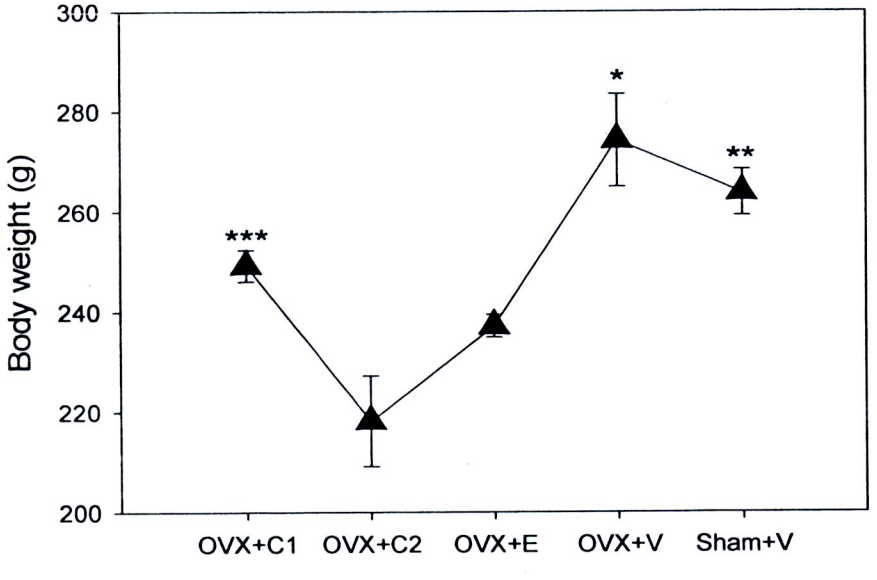

Figure 59 The body weight (mean±SEM) of each group at the day of sacrificed.

* Significantly different to OVX+E, OVX+C1 and OVX+C2 ($p<0.05$).

** Significantly different to OVX+E and OVX+C2 ($p<0.05$).

*** Significantly different to OVX+C2 ($p<0.05$).

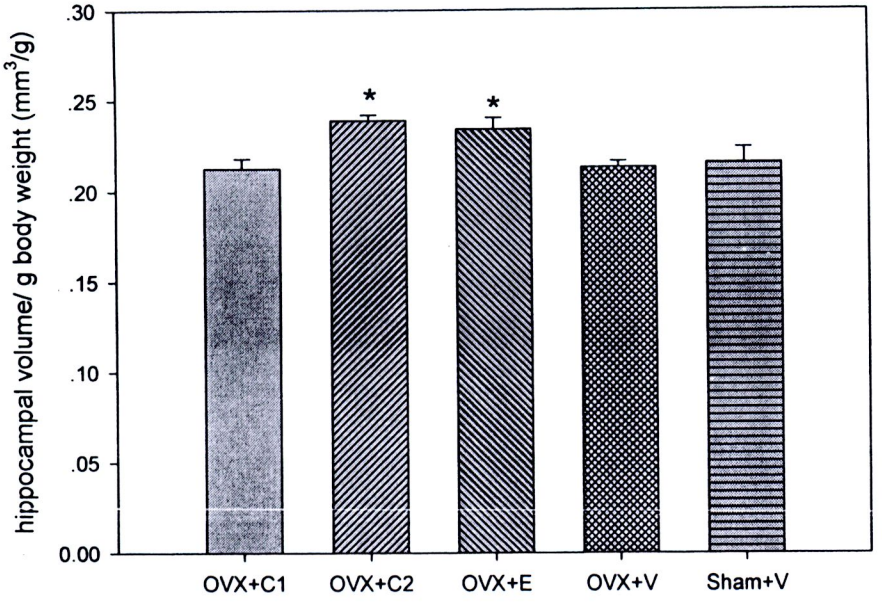

Figure 60 The hippocampus volume per gram body weight (mean±SEM) of each group.

* Significant different to OVX+C1, OVX+V and Sham+V ($p<0.05$).

4.4.4 Neuron density in CA1 and CA3 areas

a) CA1 area

The real size at 40X magnification under the microscope was 0.27×0.2 mm. All the neurons in this rectangle were counted for compared (Figure 61). The average neuron number from total slides, anterior hippocampus (1st one-third of the total slides), middle hippocampus (2nd one-third of the total slides), and posterior hippocampus (last one-third of the total slides) were compared between groups by running the ANOVA analysis. The OVX+V and OVX+E groups had the significant higher absolute neuron number in the CA1 area than that of OVX+C1, OVX+C2 and Sham+V groups ($P<0.05$), with the similar distribution in the anterior, middle and posterior hippocampus (Figure 62-65). The proportional neuron numbers to the body weight in CA1 area were compared to eliminate the factor of body weight. The OVX+E and OVX+C2 groups showed a significant higher proportional neuron density in the CA1 area than that of OVX+V, OVX+C1 and Sham+V groups. Similar

trends were observed in the anterior, middle and posterior hippocampus (Figure 66-69).

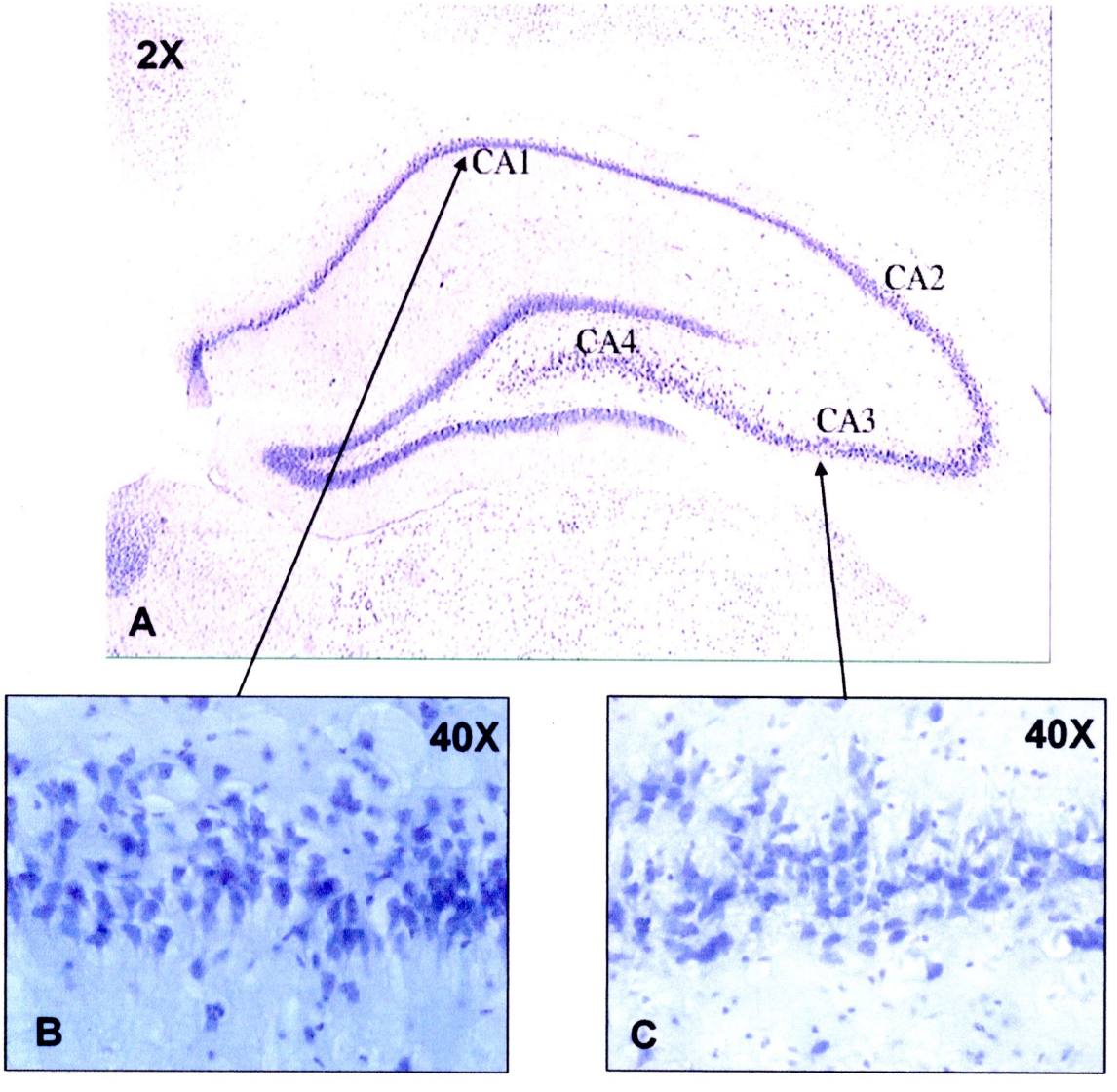

Figure 61 The Nissl staining section-hippocampal area. A: whole hippocampus under the microscope (2X). B: CA1 area (40X). C: CA3 area (40X)

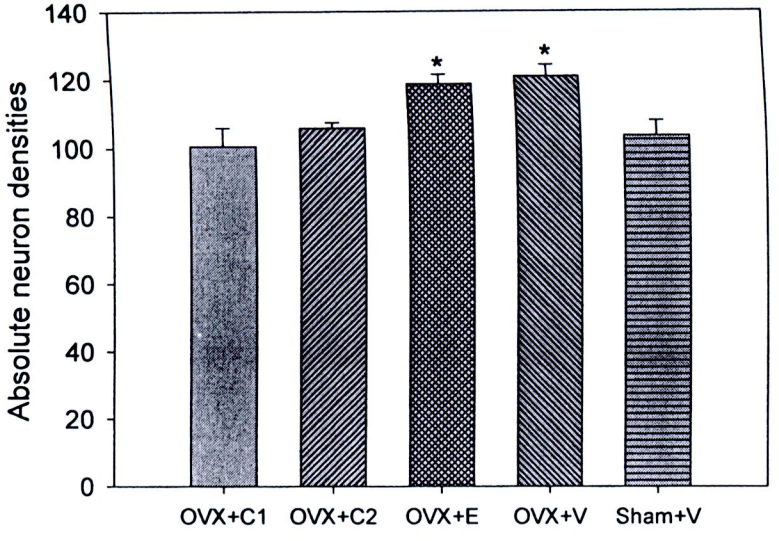

Figure 62 The absolute neuron density (mean±SEM) in CA1 area of each group.

* Significantly different to OVX+C1, OVX+C2 and Sham+V groups ($P<0.05$).

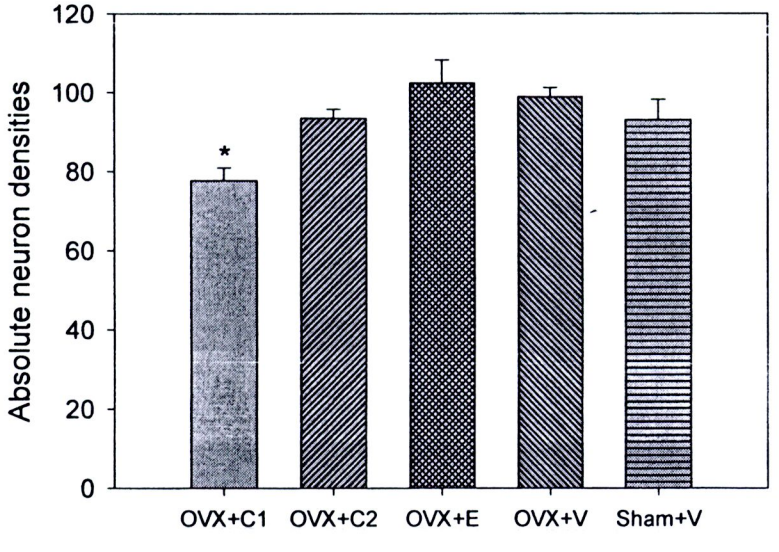

Figure 63 The absolute neuron density (mean±SEM) in CA1 area in anterior hippocampus of each group.

* Significantly different to OVX+C2, OVX+E. OVX+V and Sham+V groups ($P<0.05$).

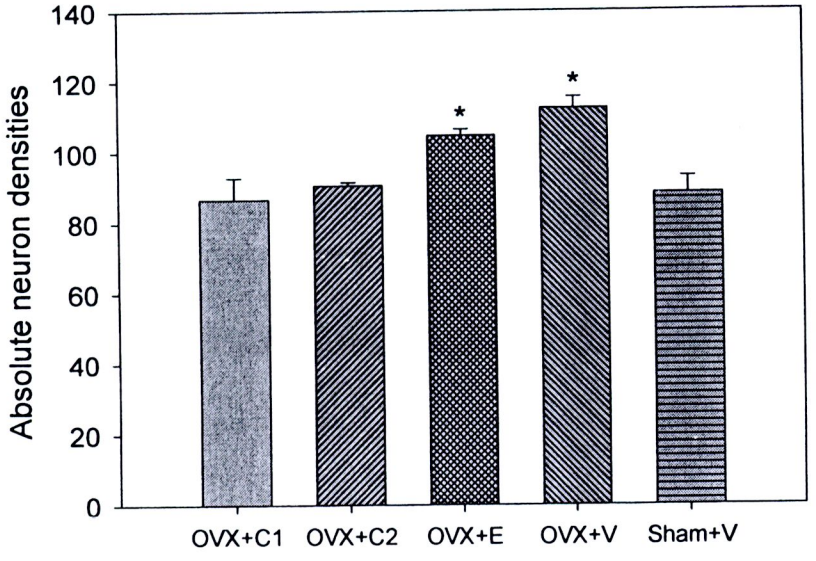

Figure 64 The absolute neuron density (mean±SEM) in CA1 area in middle hippocampus of each group.

* Significantly different to OVX+C1, OVX+C2 and Sham+V groups ($P<0.05$).

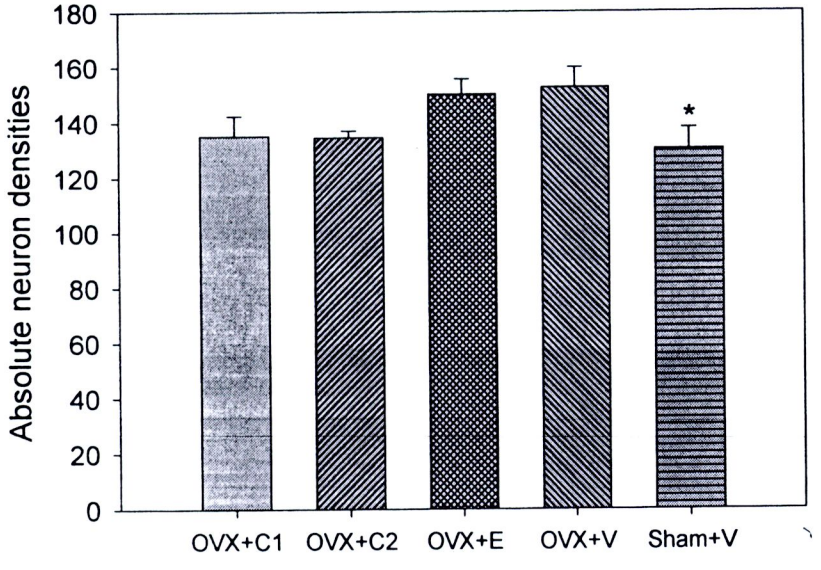

Figure 65 The absolute neuron density (mean±SEM) in CA1 area in posterior hippocampus of each group.

* Significantly different to OVX+E and OVX+V groups ($P<0.05$).

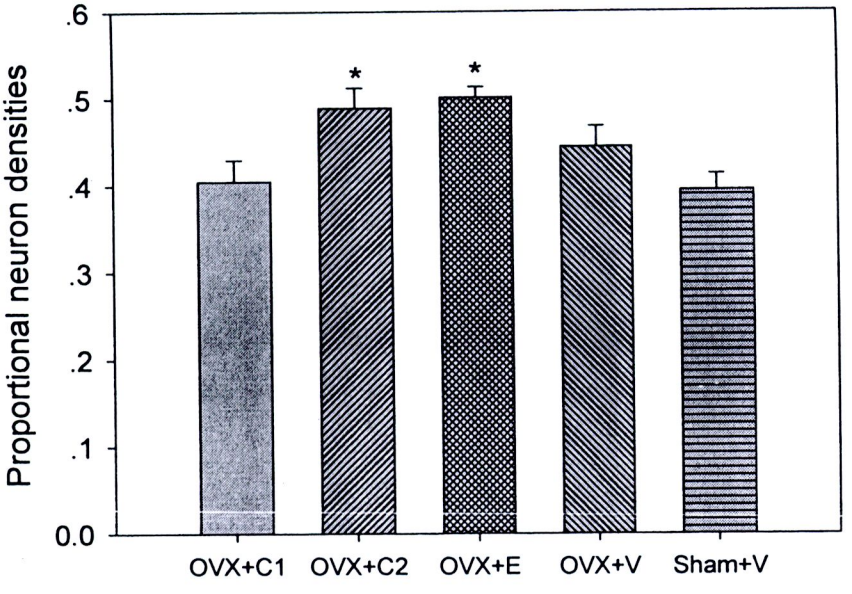

Figure 66 The proportional neuron density (mean±SEM) in CA1 area of each group.
* Significantly different to OVX+C1 and Sham+V groups (P<0.05).

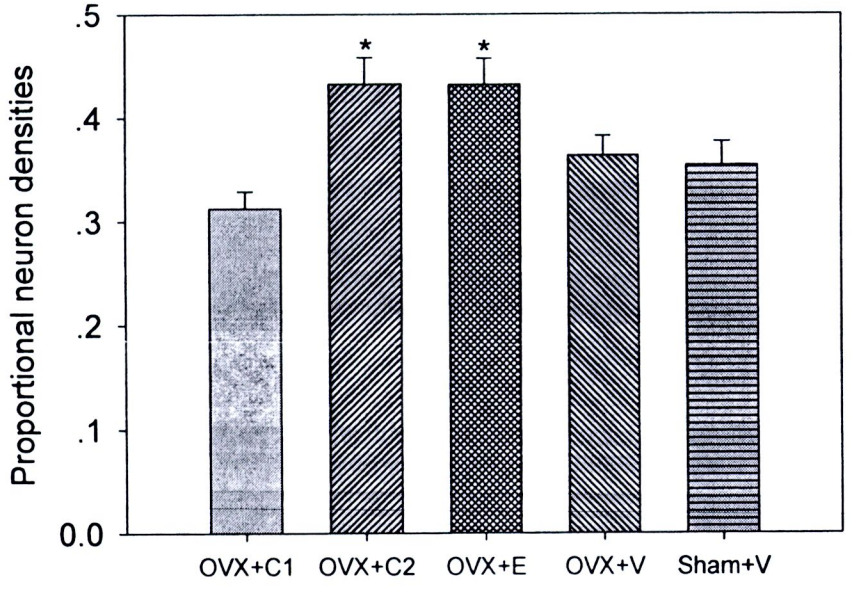

Figure 67 The proportional neuron density (mean±SEM) in CA1 area in anterior hippocampus of each group.
* Significantly different to OVX+C1, OVX+V and Sham+V groups (P<0.05).

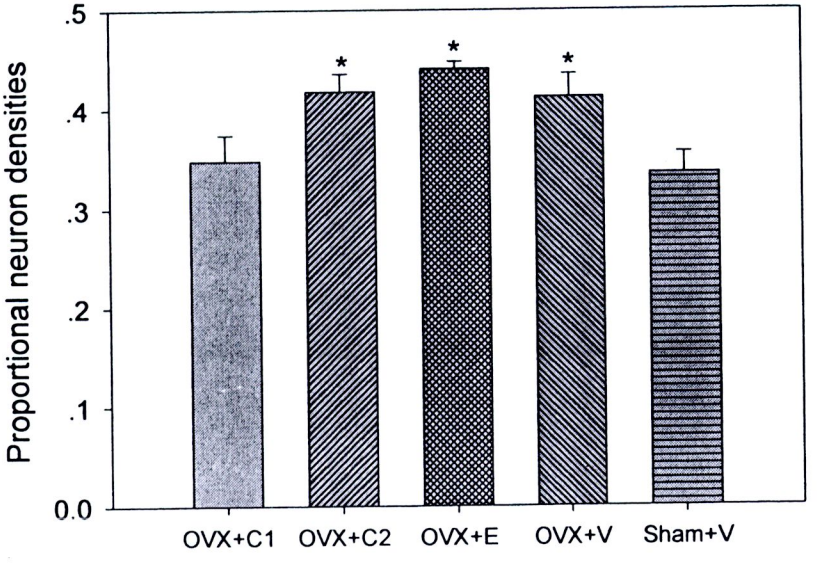

Figure 68 The proportional neuron density (mean±SEM) in CA1 area in middle hippocampus of each group.

* Significantly different to OVX+C1 and Sham+V groups ($P<0.05$).

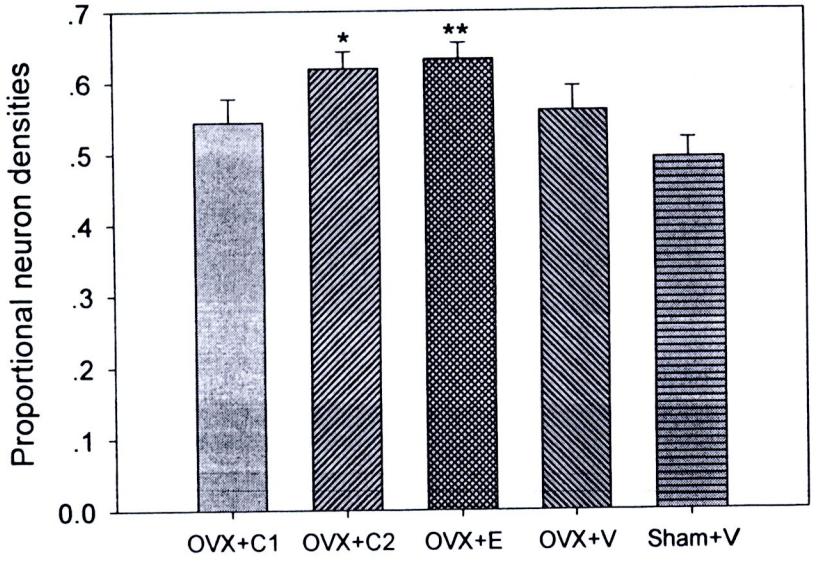

Figure 69 The proportional neuron density (mean±SEM) in CA1 area in posterior hippocampus of each group.

* Significantly different to Sham+V groups ($P<0.05$);

** Significantly different to Sham+V and OVX+C1 group ($P<0.05$).

b) CA3 area

Sham+V group had the highest absolute neuron number in the counting region, with OVX+E and OVX+C2 groups in the second level, followed by the OVX+C1 and OVX+V groups. The similar results were observed in the anterior, middle and posterior hippocampus except that OVX+C2 had the lowest neuron number in the posterior hippocampus (Figure 70-74). After compensating from the body weight, OVX+C2 group had the highest proportional neuron densities, with the OVX+E group in the second, followed by Sham+V and OVX+C1 and the OVX+V at the last. The same trends were observed in all 3 parts of hippocampus (Figure 75-77).

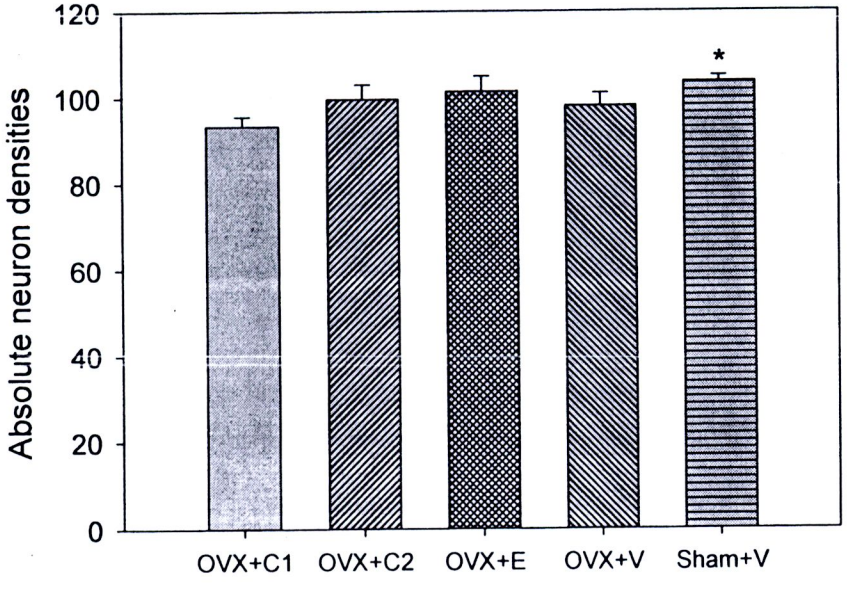

Figure 70 The absolute neuron density (mean±SEM) in CA3 area of each group.
* Significantly different to OVX+C1 groups ($P<0.05$).

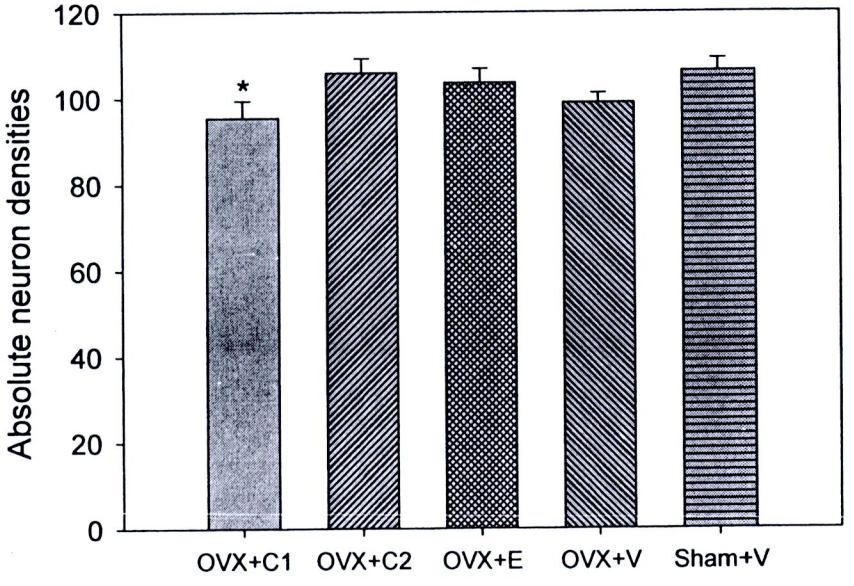

Figure 71 The absolute neuron density (mean±SEM) in CA3 area in anterior hippocampus of each group.

* Significantly different to OVX+C2 and Sham+V groups ($P<0.05$).

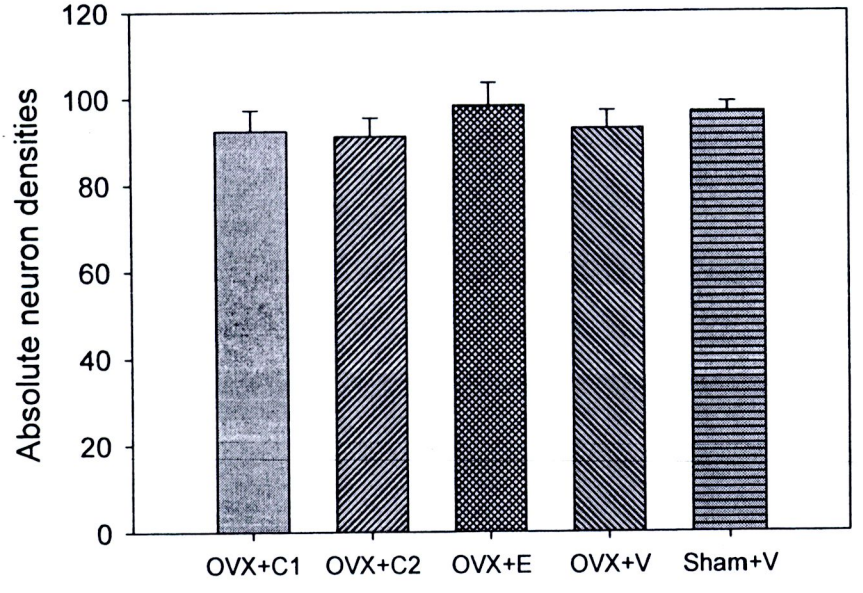

Figure 72 The absolute neuron density (mean±SEM) in CA3 area in middle hippocampus of each group. No significant difference between groups ($P>0.05$)

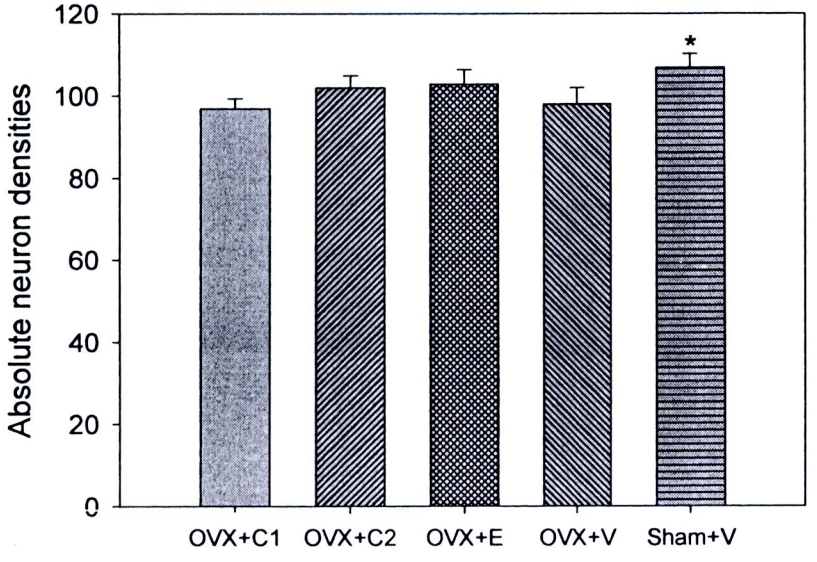

Figure 73 The absolute neuron density (mean±SEM) in CA3 area in posterior hippocampus of each group.

* Significantly different to OVX+C1group ($P<0.05$).

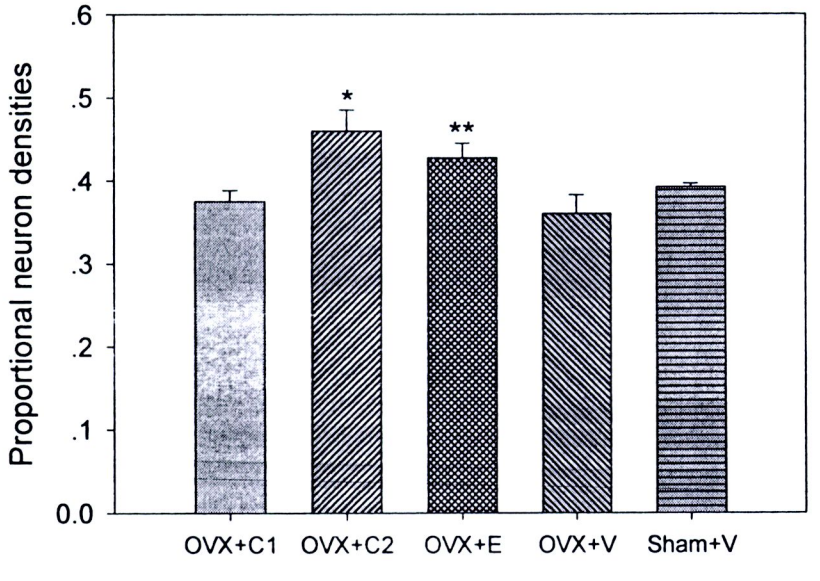

Figure 74 The proportional neuron density (mean±SEM) in CA3 area of each group.

* Significantly different to OVX+C1, OVX+V and Sham+V groups ($P<0.05$).

** Significantly different to OVX+V group ($P<0.05$).

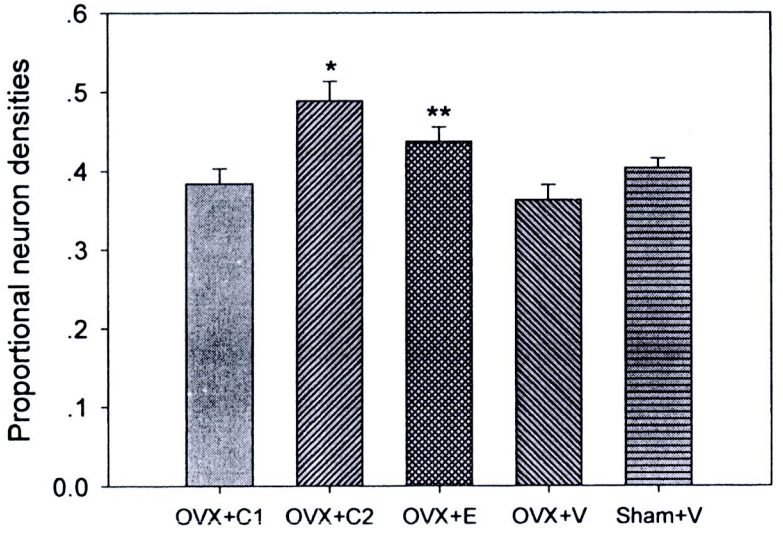

Figure 75 The proportional neuron density (mean±SEM) in CA3 area in anterior hippocampus of each group.

* Significantly different to OVX+C1, OVX+V and Sham+V groups ($P<0.05$).

** Significantly different to OVX+V group ($P<0.05$).

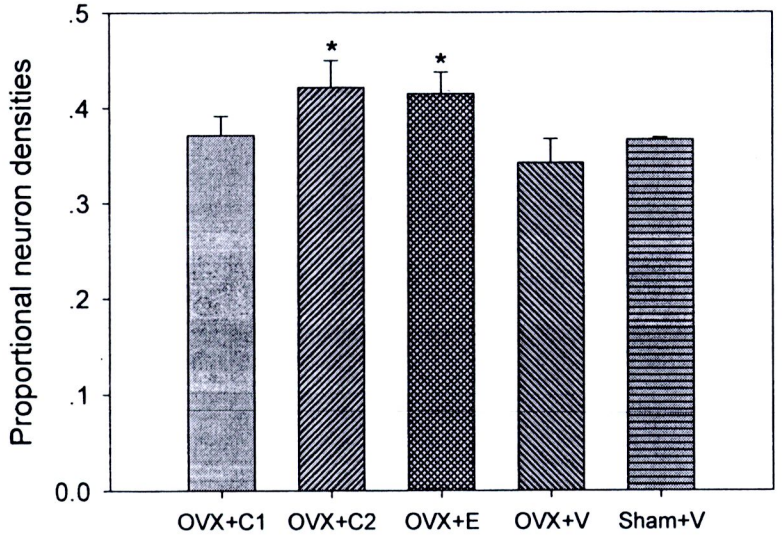

Figure 76 The proportional neuron density (mean±SEM) in CA3 area in middle hippocampus of each group.

* Significantly different to OVX+V group ($P<0.05$).

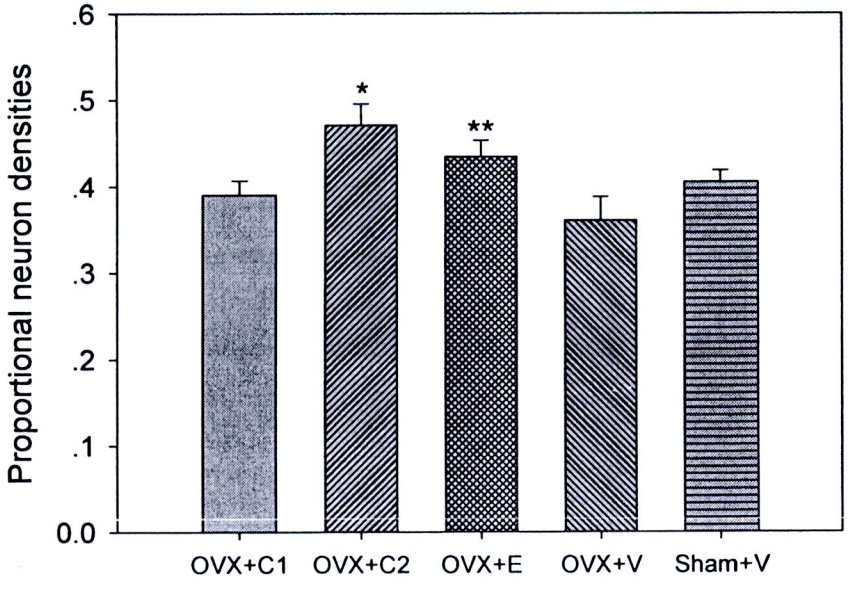

Figure 77 The proportional neuron density (mean±SEM) in CA3 area in posterior hippocampus of each group.

* Significantly different to OVX+C1, OVX+V and Sham+V groups ($P<0.05$).

** Significantly different to OVX+V group ($P<0.05$).

4.5 The effect of the CHE on the antioxidative enzyme activities in the rat brain against ethanol-induced oxidative stress

4.5.1 Catalase (CAT) activities

The influence of administration of alcohol and the CHE to the CAT in the brain was observed in different regions.

CAT activity in the pituitary was the highest compared to the other tissues (Figure 78). In the hypothalamus, CAT activity increased in the EtOH group compared to the normal group. The treatment of CHE at low dose slightly decreased the CAT activity but the high dose did not. In contrast, the treatment of CHE at both doses without ethanol significantly decreased the CAT activity compared to the EtOH and EtOH+C2 groups (Figure 79).

The coordinated effects of alcohol and CHE were also found in the other tissues. In the hippocampus, EtOH+C1 and EtOH+C2 groups had more obvious decrease of the CAT activity while the less decrease in the C1 and C2 groups compared to the alcohol treated group (Figure 80). Reversed effects was found in the cortex and cerebellum, where the co-treated of alcohol and CHE increased the CAT activity (Figure 81-82).

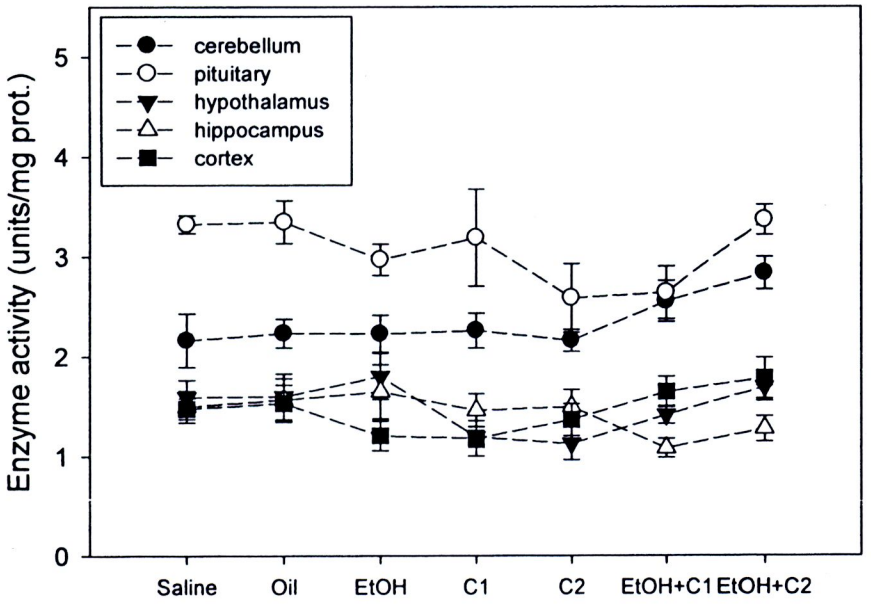

Figure 78 The CAT activities (mean±SEM) in cerebellum, pituitary, hypothalamus, hippocampus and cortex of each group.

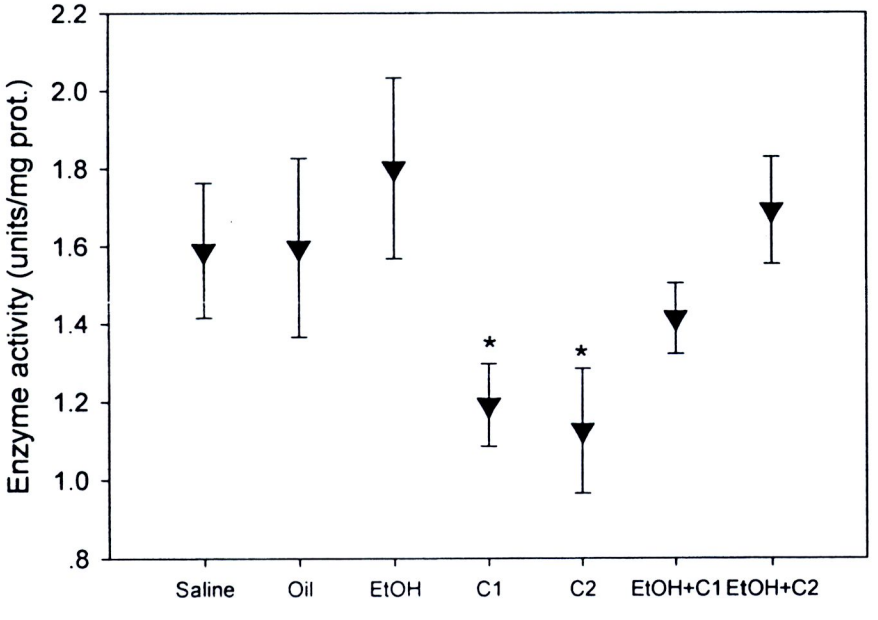

Figure 79 CAT activity (mean±SEM) in the hypothalamus of each group.
* Significant different to EtOH and EtOH+C2 groups ($P<0.05$).

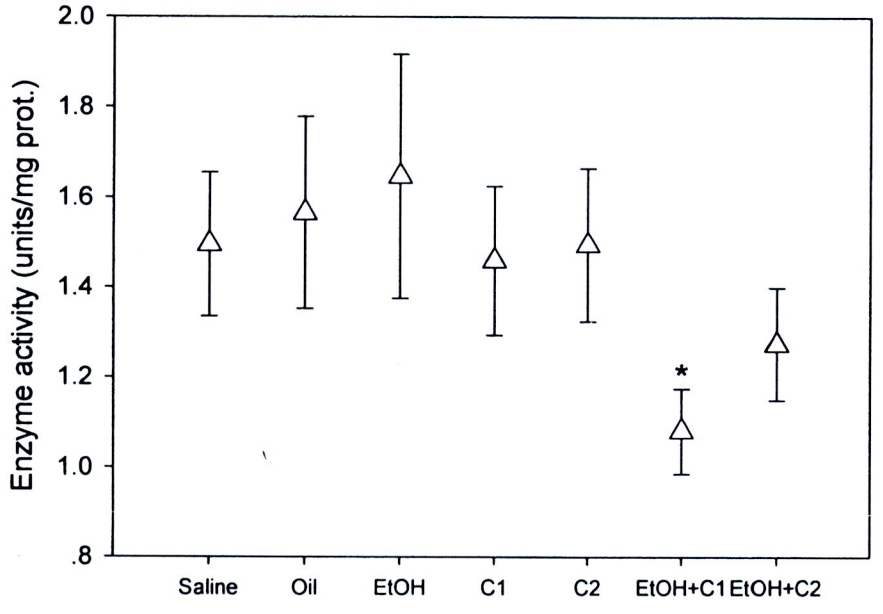

Figure 80 CAT activity (mean±SEM) in the hippocampus of each group.
* Significantly different to EtOH group (P<0.05).

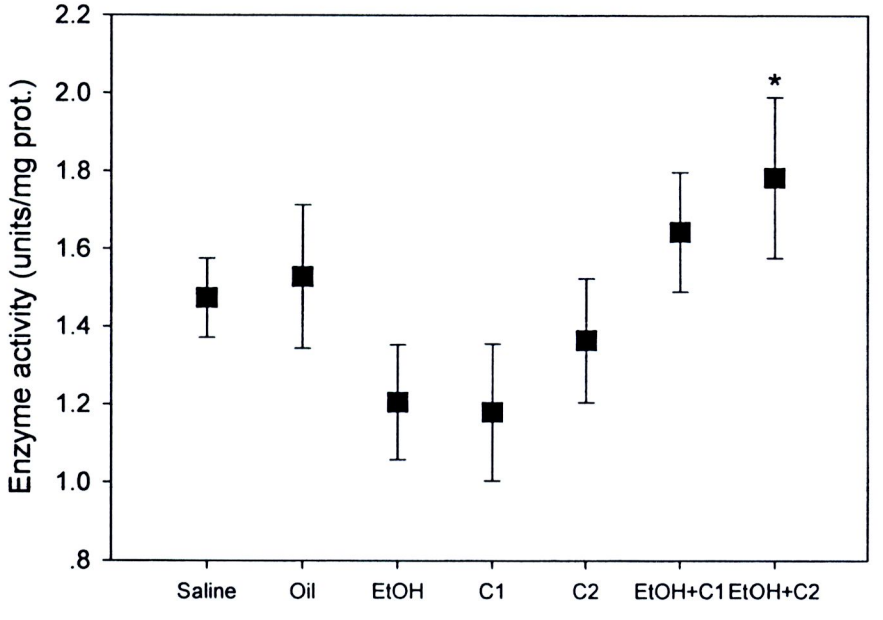

Figure 81 CAT activity (mean±SEM) in the cortex of each group
* Significantly different to EtOH and C1 groups (P<0.05).

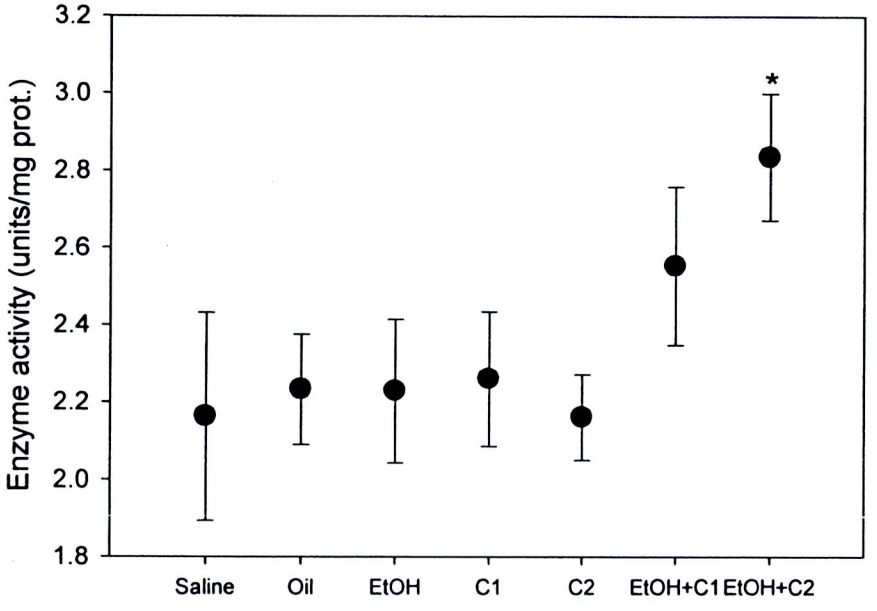

Figure 82 CAT activity (mean±SEM) in the cerebellum of each group.
* Significantly different to Saline, Oil, EtOH, C1 and C2 groups ($P<0.05$).

4.5.2 Superoxide dismutase (SOD) activities

SOD activity in the cortex was the highest compared to the other tissues (Figure 83). The proportions of the SOD activity of each tissue were quite similar in different groups. Alcohol treatment slightly increased the SOD activity in all the tissues. CHE and alcohol co-treatment augmented the increase of the SOD activity in the brain. Similar increased effect was observed in the low dose CHE treated group but not in the high dose group.

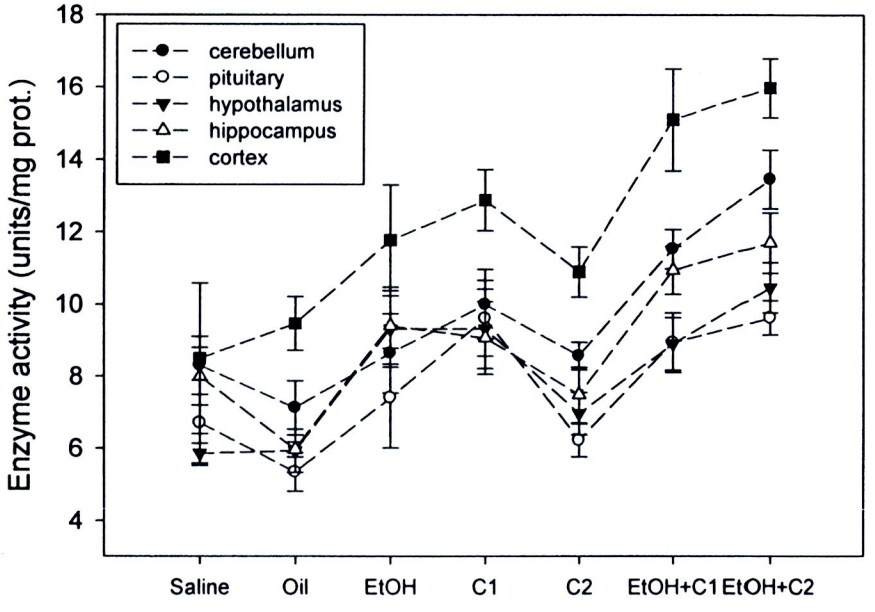

Figure 83 The SOD activity (mean±SEM) in cerebellum, pituitary, hypothalamus, hippocampus and cortex of each group.

4.5.3 Glutathione peroxidase (GPx) activities

GPx activity in the pituitary was highest compared to the other tissues (Figure 84). Higher GPx activity was found in the alcohol treated group in hypothalamus and hippocampus. This effect was reversed by the CHE co-treatment in both high and low doses (Figure 85-86). The co-treatment of alcohol and CHE also decreased the GPx activity in the cerebellum. It was unexpected that high dose of CHE itself also decreased the GPx activity in the cerebellum (Figure 87).

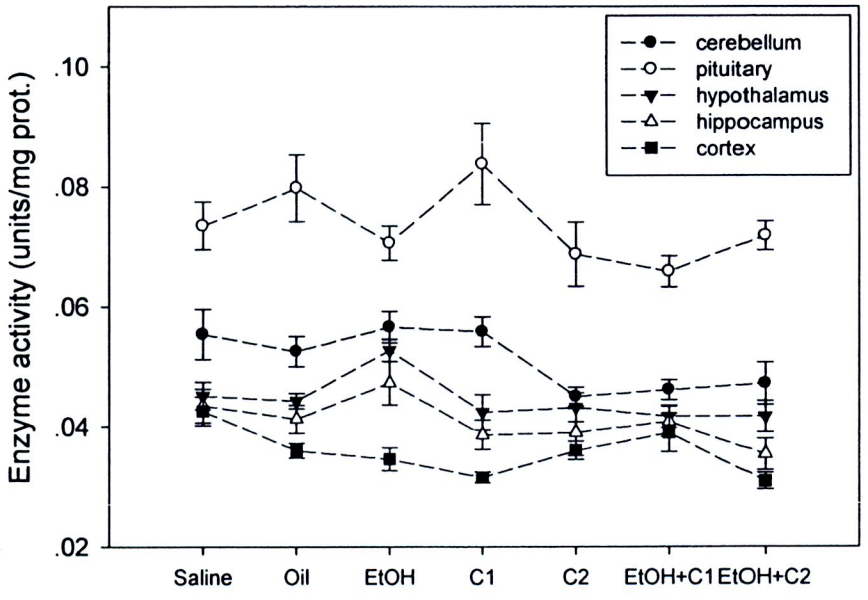

Figure 84 The GPx activity (mean±SEM) in cerebellum, pituitary, hypothalamus, hippocampus and cortex of each group.

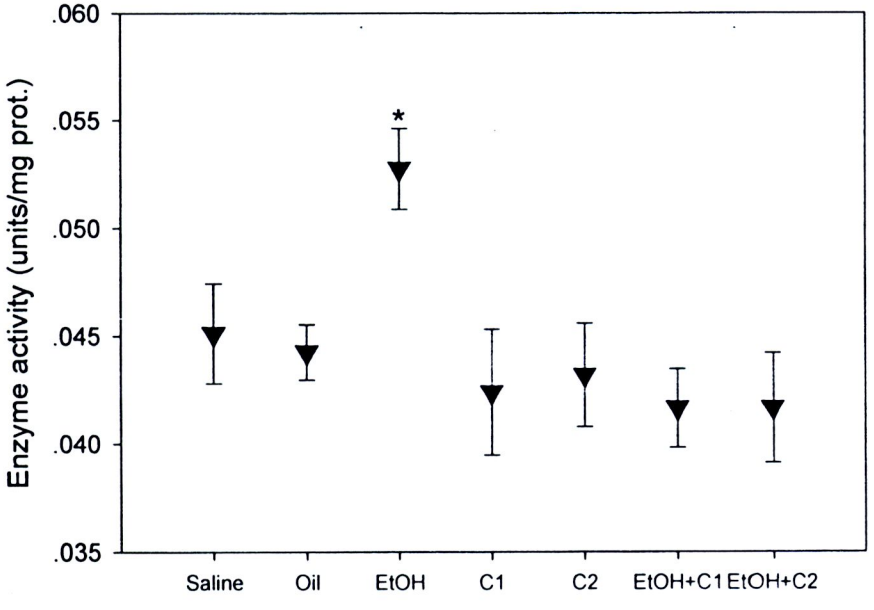

Figure 85 GPx activities (mean±SEM) in the hypothalamus of each group.

* Significantly difference to the other 5 groups ($P<0.05$).

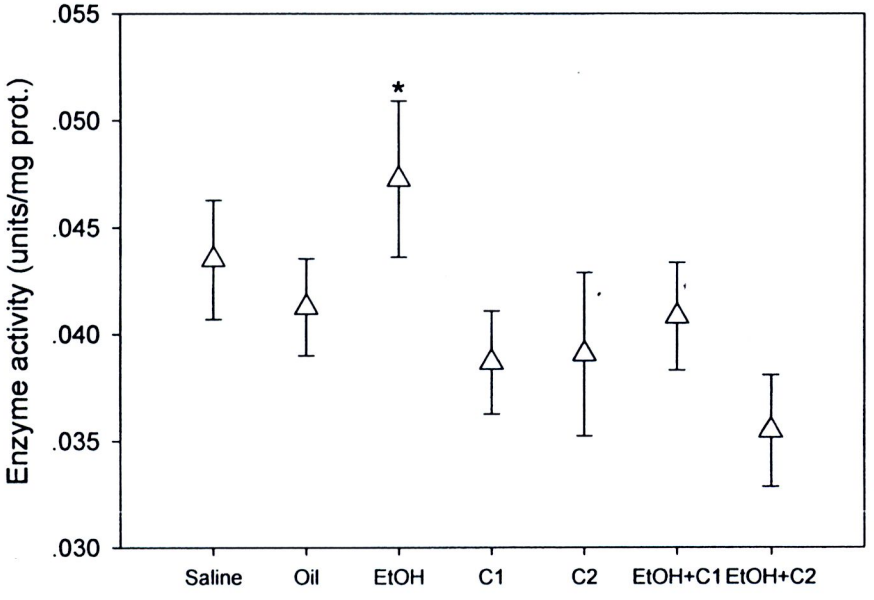

Figure 86 GPx activity (mean±SEM) in the hippocampus of each group.

* Significantly different to C1 and EtOH+C2 groups ($P<0.05$)

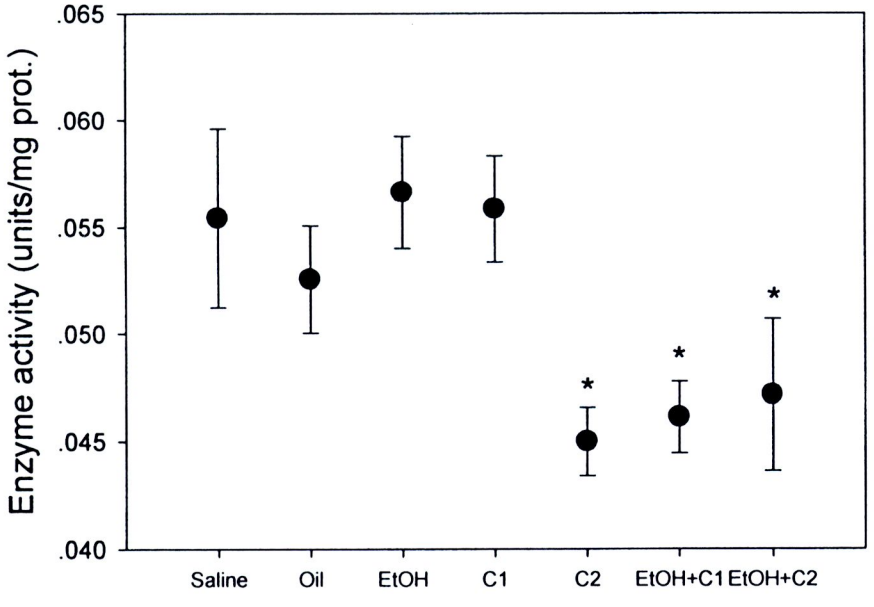

Figure 87 GPx activity (mean±SEM) in the cerebellum of each group.

* Significantly different to Saline, Oil, EtOH and C1 groups ($P<0.05$).

4.6 The pharmacokinetic study of the CHE

4.6.1 Compound separation

Under the current HPLC analysis system, CHE was separated into 13 peaks. The peaks were named as peak 1 to peak 13 as their retention time increased (Figure 88). The related compounds were named as compound 1 to 13. The purpose for developing these HPLC system was to separate the compounds in the crude extract from each other as many as we could. Both reversed phase system and normal phase system had been tested. Finally the normal phase system was selected since the non-polar characteristics of the hexane extract. The ratio of dichloromethane and hexane was varied and some located solvents such as methanol was added to optimize the separation. Higher hexane percentage would produce the better separation. Considering the runtime of each analysis, the ratio of dichloromethane and hexane was set at 6:4.

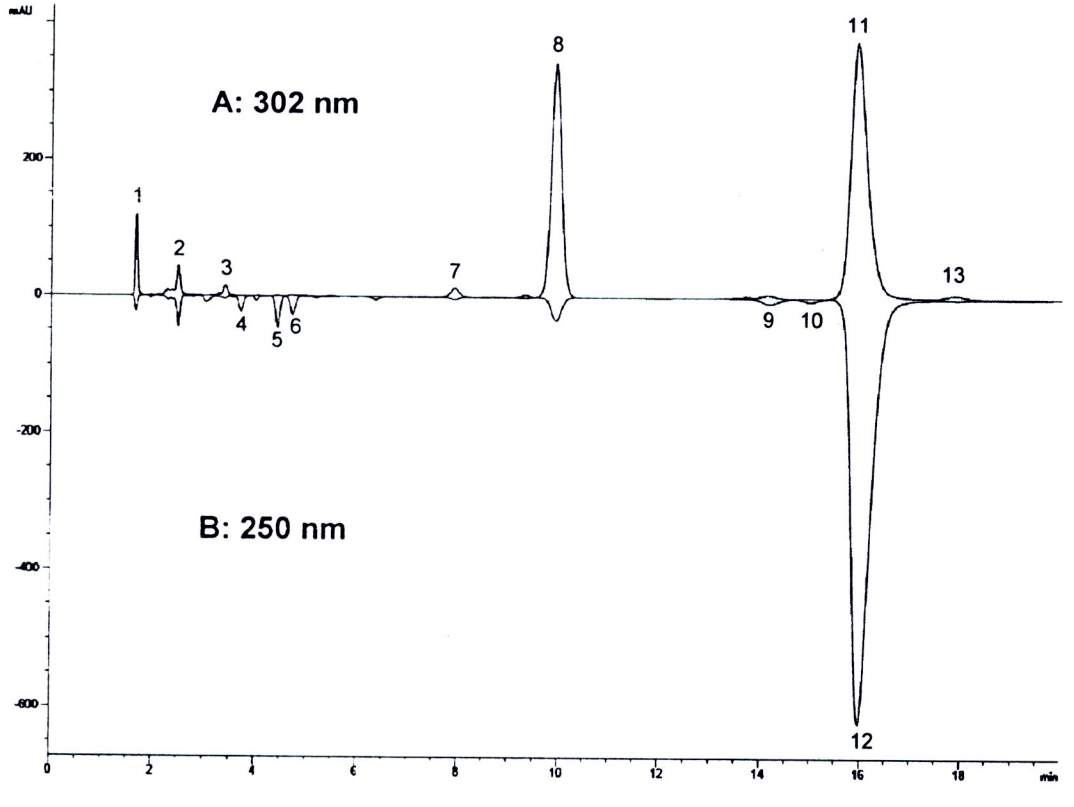

Figure 88 HPLC chromatogram of CHE (1 mg/ml) at 302 nm (A) and 250 nm (B). Thirteen peaks were found and numbered from 1 to 13 to represent the relative compounds with the time they flowed out from the column.

The chromatogram of the purified compound, 1,7-diphenyl-5-hydroxy-(1E,3E)-1,3-hepttadiene is shown as Figure 89

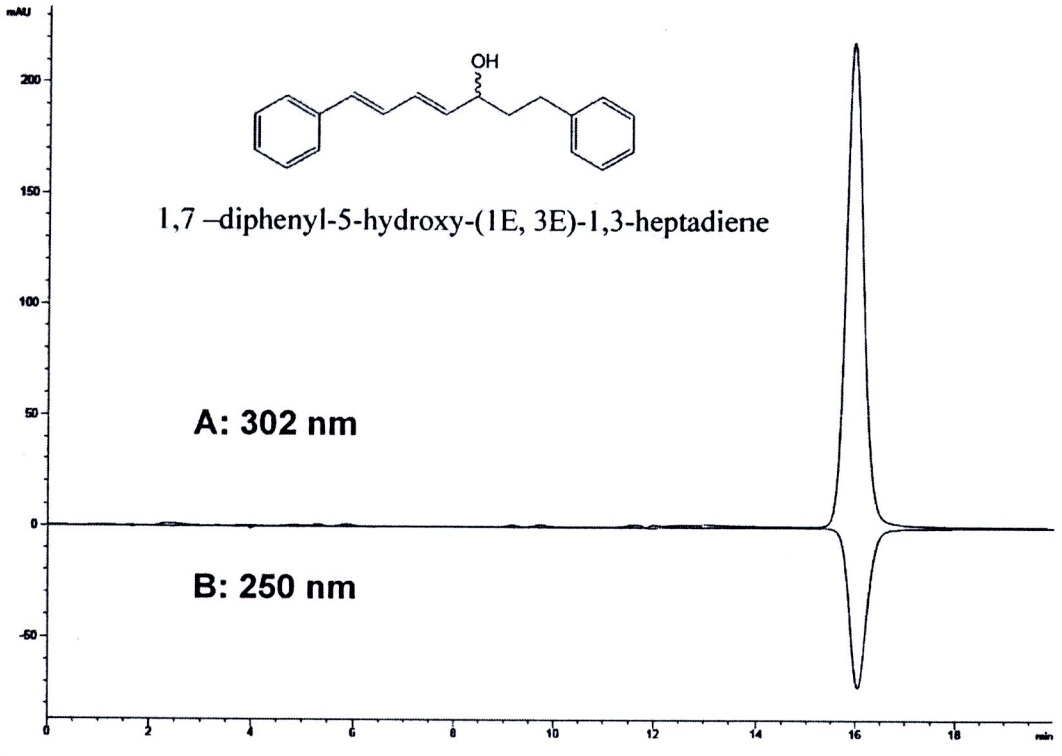

Figure 89 HPLC chromatogram of 1,7-dipheny-5-hydroxy-(1E,3E)-1,3-heptadiene (0.1 mg/ml) at 302 nm (A) and 250 nm (B).

4.6.2 HPLC method validation

a) Wavelength selection

The peak patterns of CHE detected under different wavelength (210 nm to 390 nm) are shown in Figure 90. The combination of the detected wavelength of 302 nm and 250 nm showed the most peaks and clear pattern when compared to the others, which could represent the crude extract in the best way.

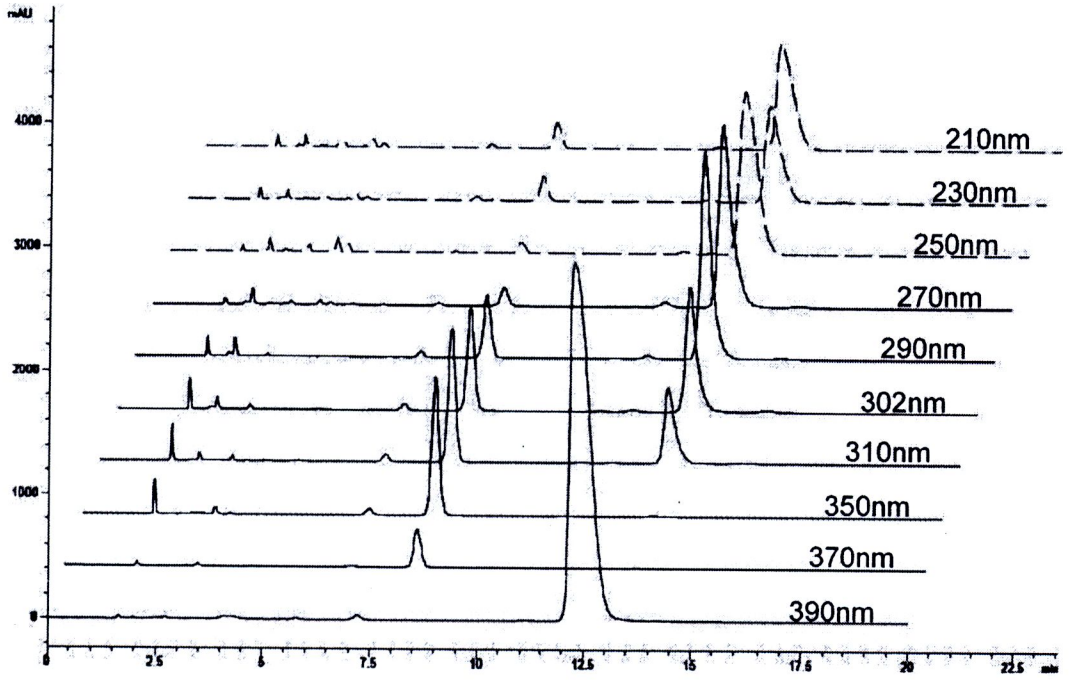

Figure 90 Chromatogram of CHE extract (1 mg/ml) at the wavelength from 210 to 390 nm. The wavelength at 250 and 302 nm were selected for analyzing the samples.

b) Precision and stability

The area of each peak detected at 302 nm in the same day is shown at Table 27. The %CV range from 0.61 to 6.44 indicated an acceptable precision for analysis. The CHE sample was stable in the mobile phase at room temperature within 24 hours (Table 28)

Table 27 The precision analysis of CHE by HPLC method

	Peak Area					
	Peak1	Peak2	Peak3	Peak7	Peak8	Peak11
test 1	37.6	18.9	8.4	18	508.8	897.7
test 2	38.4	19.1	8.5	17.3	510.4	904.2
test 3	38.6	19.1	8.5	19.6	510.3	910.1
Average	38.20	19.03	8.47	18.30	509.83	904.00
SD	0.53	0.12	0.06	1.18	0.90	6.20
CV (%)	1.39	0.61	0.68	6.44	0.18	0.69

Table 28 Stability study of CHE sample

	Peak Area					
at 0 hours	Peak1	Peak2	Peak3	Peak7	Peak8	Peak11
sample 1	562	298.2	150.8	273.5	7836.5	14159
sample 2	578.2	306.2	157.6	264.1	8056.3	14487.7
sample 3	595.7	327.4	147.2	271	8604.7	15397
Average	578.63	310.60	151.87	269.53	8165.83	14681.23
SD	16.85	15.09	5.28	4.87	395.64	641.29
CV (%)	2.91	4.86	3.48	1.81	4.85	4.37
24 hours later						
sample 1	582.6	315.8	153.8	270.7	7940.6	15265.2
sample 2	576.3	322	146.2	266	8089.2	15481.3
sample 3	580.1	318.5	155.5	267	8744.5	16064.5
Average	579.67	318.77	151.83	267.90	8258.10	15603.67
SD	3.17	3.11	4.95	2.48	427.74	413.46
CV (%)	0.55	0.98	3.26	0.92	5.18	2.65

c) Specificity

The current method was specific as no interference was found from the drug-free tissues and the olive oil (Figure 91-92). At 302 nm the brain, ovary and uterus extract had a peak overlapped with peak 3. The olive oil had a peak overlapped with peak 2. The measurement of these peaks was excluded in the tissues.

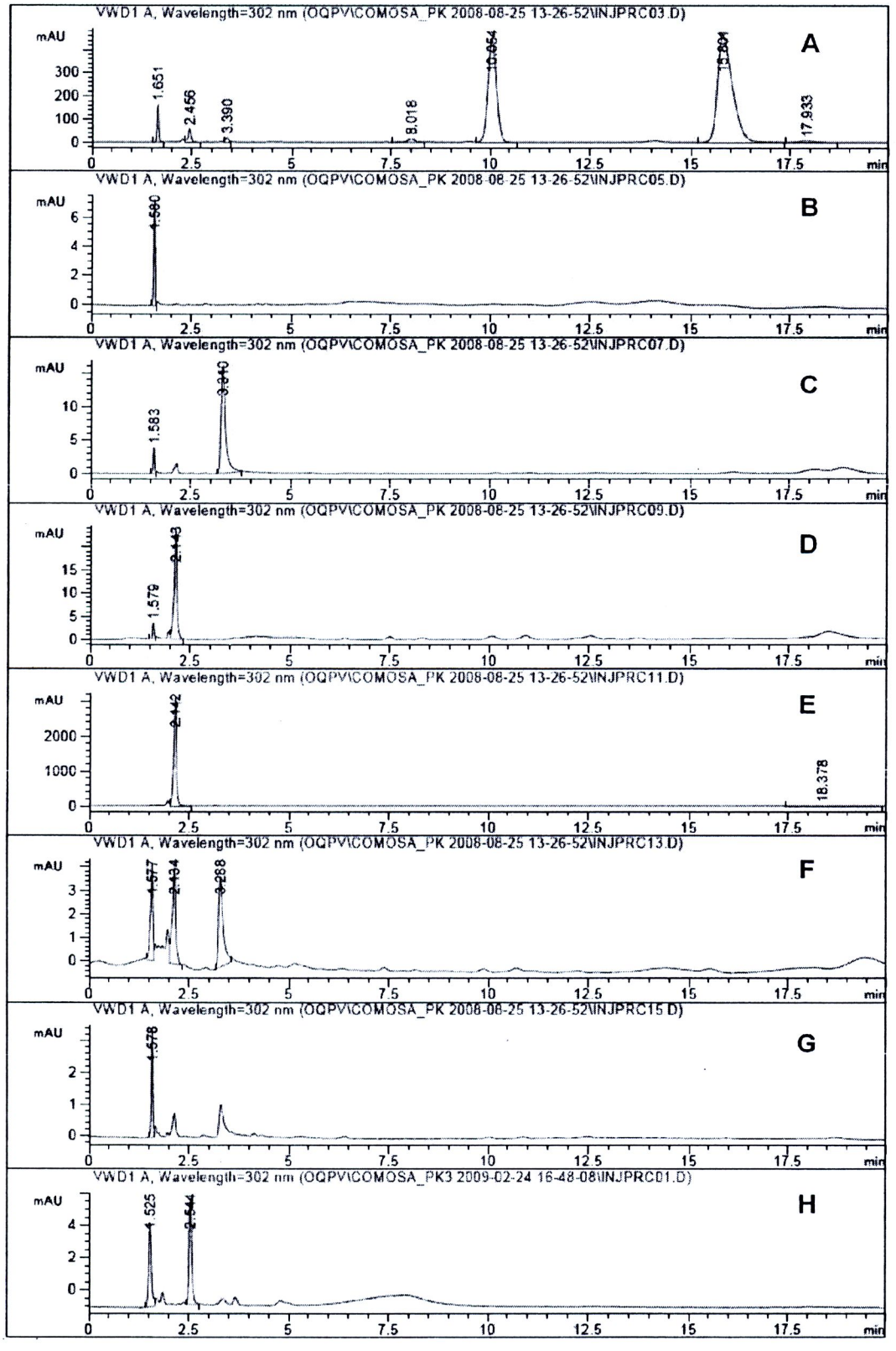

Figure 91 HPLC chromatograms at 302 nm. 1 mg/ml CHE (A), 45 mg/ml olive oil (H) and blank tissue samples including blood (B), brain (C), kidney (D), liver (E), ovary (F) and uterus (G).

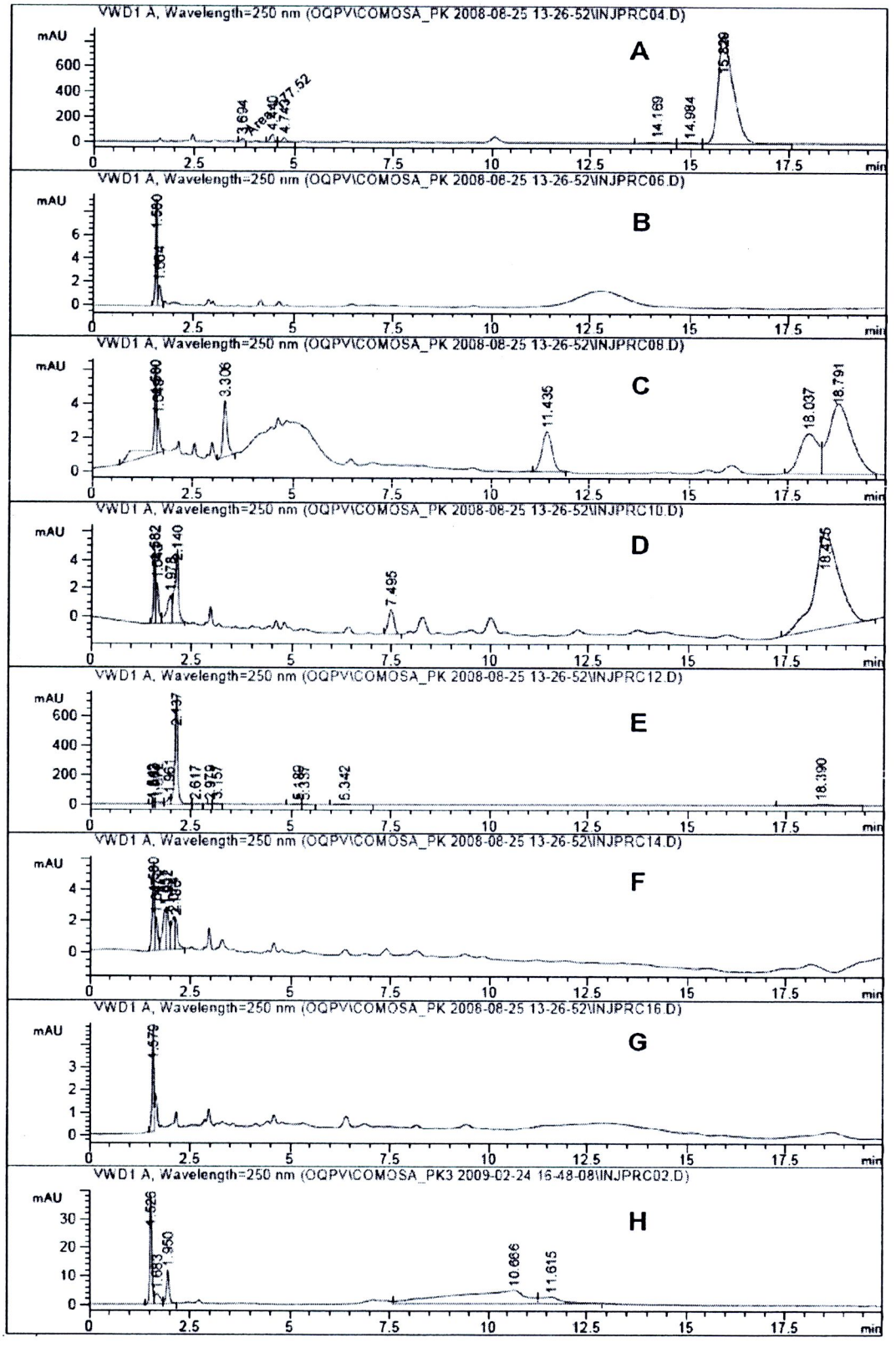

Figure 92 HPLC chromatograms of CHE at 250 nm. 1 mg/ml CHE (A), 45 mg/ml olive oil (H) and blank tissue samples including blood (B), brain (C), kidney (D), liver (E), ovary (F) and uterus (G).

d) *Linearity*

The method was found to be linear over a range of 0.001-5.0 mg/ml of CHE (Table 29).

Table 29 The calibration of correlation coefficients.

	Peak Area					
Conc(mg/ml)	Peak1	Peak2	Peak3	Peak7	Peak8	Peak11
0.001	3.1			2.25	15.95	32.05
0.01	13.45	4.85	2.75	18.3	134.05	263.3
0.05	46	22.05	10.35	54.4	529.6	1003.4
0.5	306.45	158.8	69.05	247.2	3884.35	7242.85
5	2322.55	1262.6	529.4	1208.3	30797.05	54567.45
R2	0.9992	0.9995	0.9993	0.9905	0.9994	0.9991
slope	460.2	249.96	104.54	234.21	6116.5	10821
intercept	26.48	14.625	7.75	45.6	269.46	587.25

e) *Recovery*

Recovery of peak1, 2, 3, and 11 at 302 nm were ranged from 95.5%-105.1%, which was acceptable for analysis. The peak 7 and 8 were found to have the abnormal recovery which might be due to their unstable characteristics in the blood (Table 30).

Table 30 The calibration of recovery of each peak of CHE in the blood sample.

	Peak Area					
Extract	Peak1	Peak2	Peak3	Peak7	Peak8	Peak11
sample 1	37.6	18.9	8.4	18	508.8	897.2
sample 2	38.4	19.1	8.4	17.3	510.4	904.2
sample 3	38.6	19.1	8.5	19	510.3	910.1
Average	38.20	19.03	8.43	18.10	509.83	903.83
In the blood						
sample 1	34.5	16.3	9.3	46.1	395.9	785.2
sample 2	41.6	19.7	9.1	64.7	465.2	946.8
sample 3	37.9	17.9	8.2	57.2	423.8	858.6
Average	38.00	17.97	8.87	56.00	428.30	863.53
Recovery (%)	0.995	0.944	1.051	3.094	0.840	0.955

4.6.3 Pharmacokinetics parameters of CHE

The sample from I.V and oral feeding groups was analyzed by HPLC at 302 and 250 nm. All 13 peaks were found in blood and other tissue samples of I.V groups. In oral feeding groups, only 4 peaks, including peak 1, peak 5, peak 11 and peak 12, were detected in blood and tissue samples. The peak areas of the 4 compounds in the blood related to these 4 peaks was recorded to make the concentration-time curves (Figure 93-94). The area under the curve (AUC) was calculated by the Sigmaplot (V 11.0) and compared between those obtained from oral feeding groups and I.V groups to generate the bioavailability (Table 31). The bioavailabilities of these 4 compounds were 55.50%, 26.90%, 19.27% and 25.48% respectively. All 4 compounds had their C_{max} at around 2.5 hour after oral feeding. The clearance time in the I.V group was around 12 hours.

Table 31 Bioavailability of 4 compounds obtained from oral feeding and I.V groups

	Peak1	Peak5	Peak11	Peak12
AUC(Oral)	7.86	37.32	54.57	226.91
AUC(I.V.)	14.17	138.74	283.23	890.66
Bioavailability	55.50%	26.90%	19.27%	25.48%

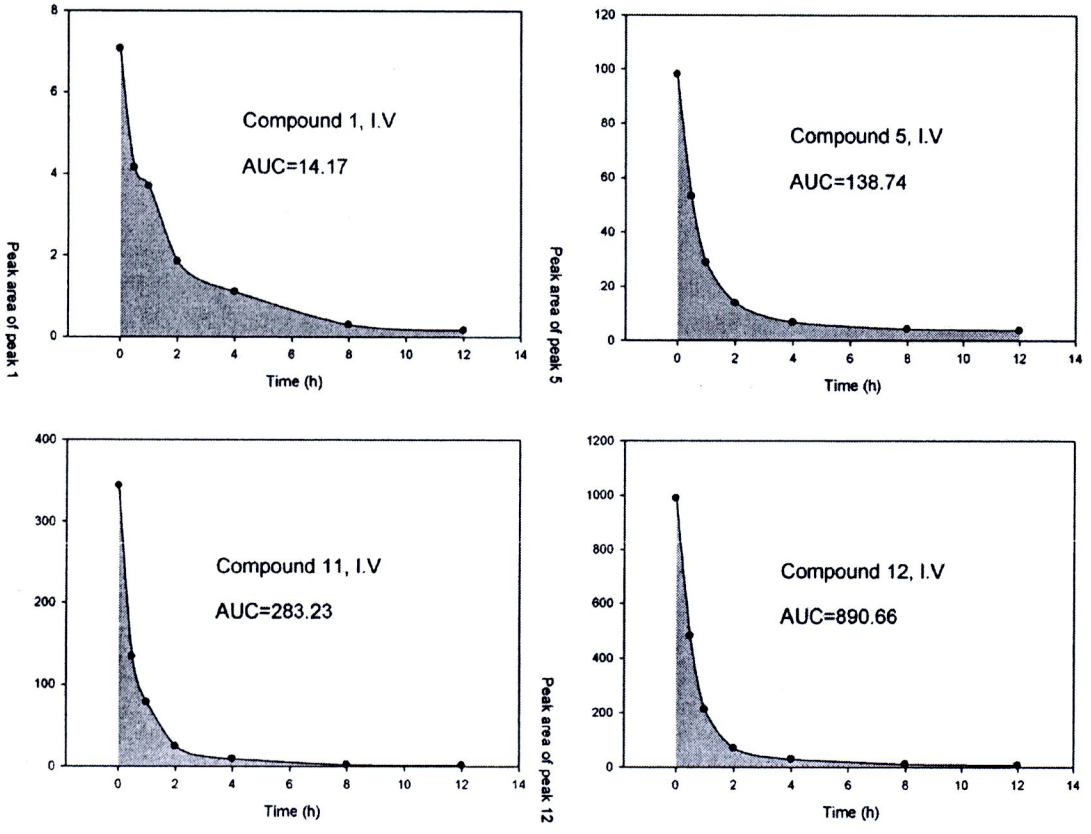

Figure 93 The concentration time curve and the AUC of compounds 1, 5, 11, 12 after the intravenous injection of CHE at a dose of 125 mg/kg body weight.

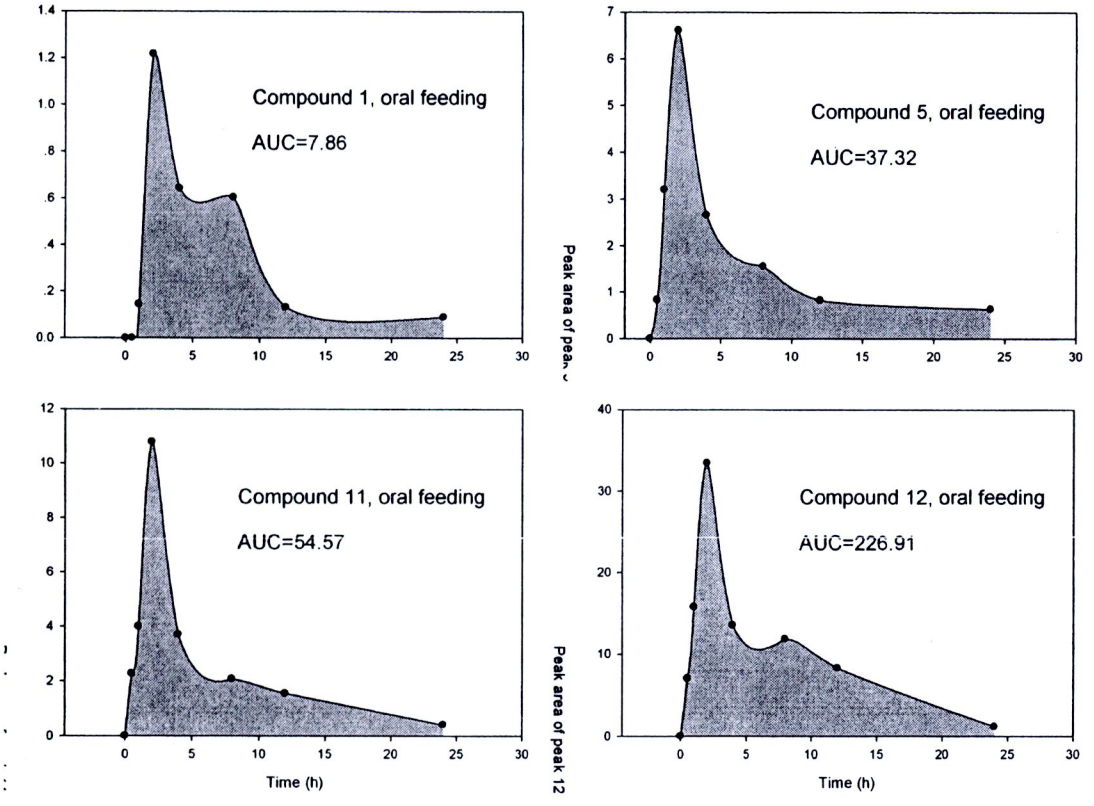

Figure 94 The blood concentration time curve and the AUC of compounds 1, 5, 11, 12 after the oral feeding of CHE at a dose of 125 mg/kg body weight.

4.6.4 The distribution of CHE in organs

The peak area of these 4 compounds in other tissues was recorded to make the concentration time curve to show the distribution in each organ (Figure 95-96). All 4 compounds were found to distribute in the brain, kidney, liver, ovary and uterus. The percentage of 4 compounds in the same organ was compared by using the peak area. From high to low were in the sequence of compound 12, 11, 5 and compound 1 in the tissues except that compound 1 expressed higher percentage than compound 5 in the brain. The compound reached their highest concentration in each organ at different times, which normally slower than the time in the bloods. The compound had a longer clearance time from ovary and uterus than other tissue or organs.

When compared the distribution of each compound in different organs, liver had the highest distribution of compound 11 and 12. Ovary was the second high distributed organ for compound 11 and 12. Compound 1 and 5 were also interesting,

while they had the highest distribution in the ovary along with a slow clearance indication the high affinity of these two compounds to the reproductive systems. Compound 1 also had the high distribution in the brain.

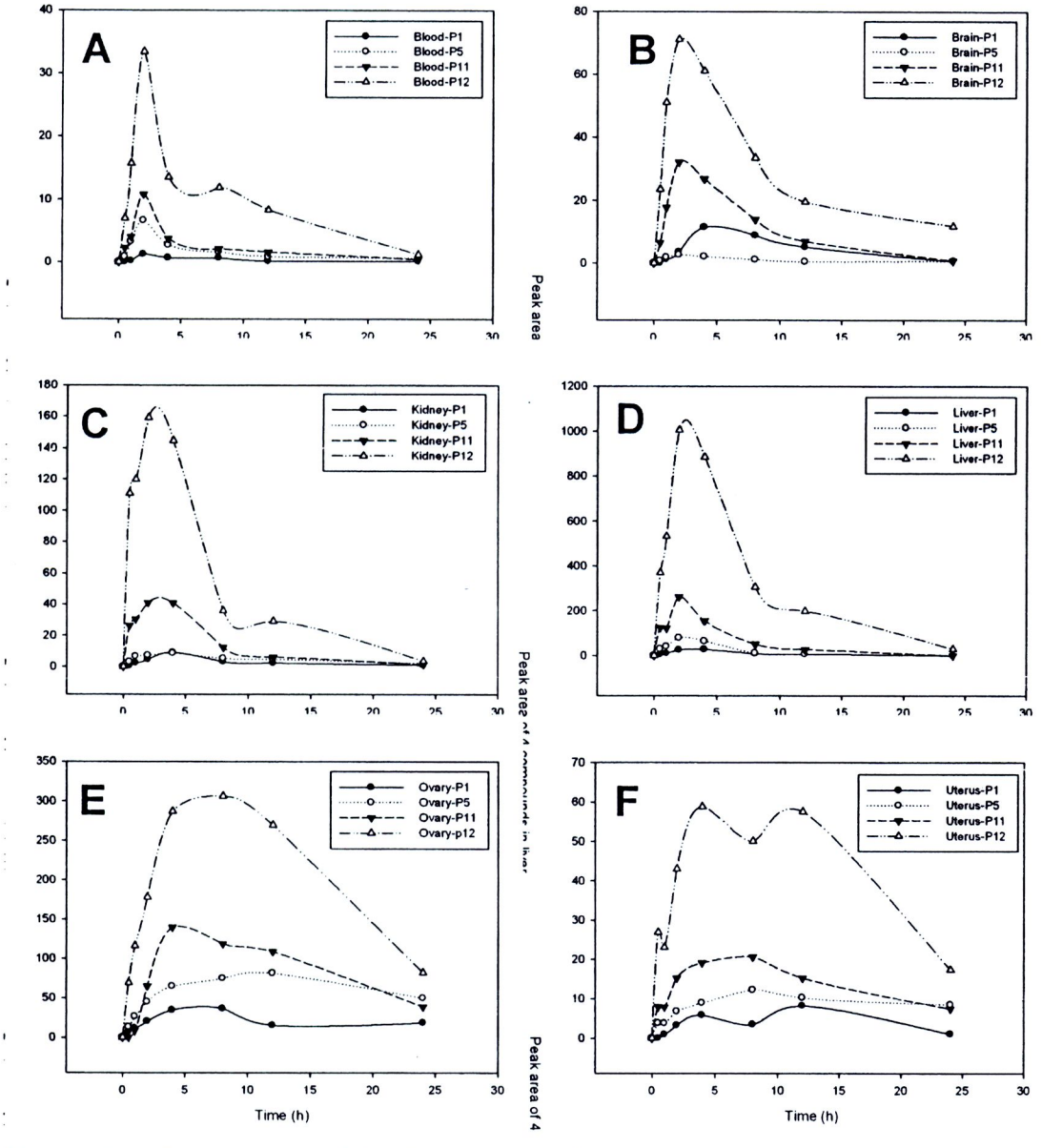

Figure 95 Comparison of the distribution of 4 compounds in the same tissue after oral feeding. A: blood; B: brain; C: kidney; D: liver; E: ovary; F: uterus.

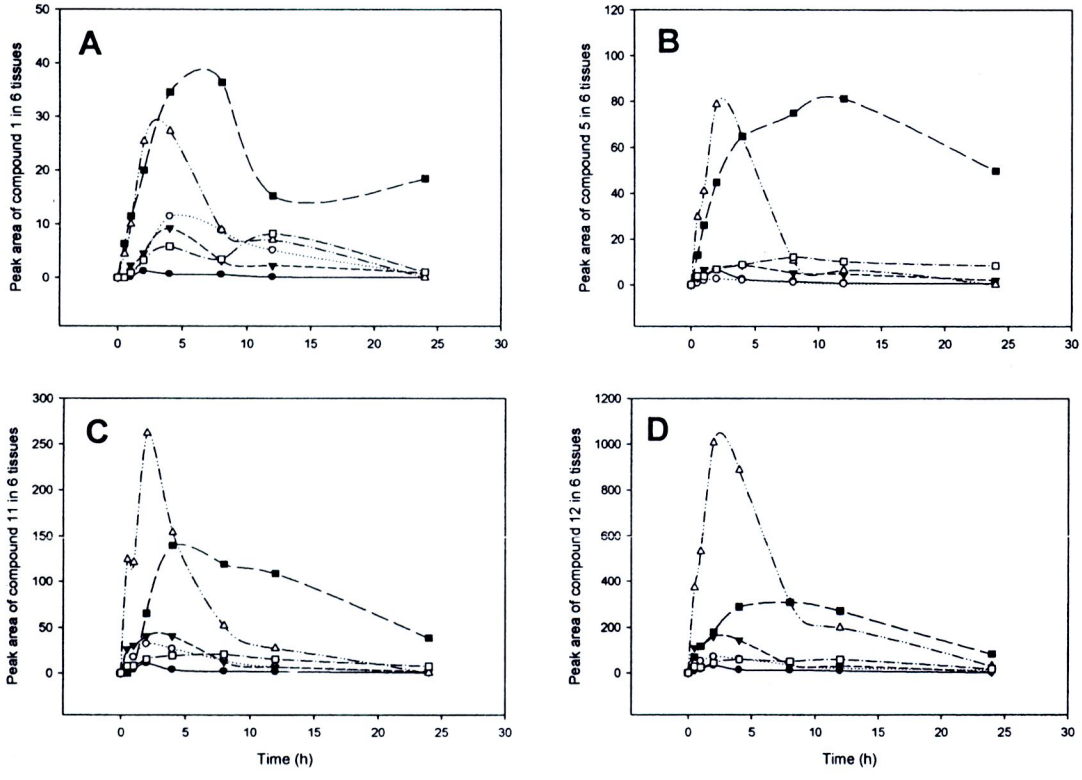

Figure 96 Comparison of each compound distribution in different tissues after oral feeding. A: compound 1; B: compound 5; C: compound 11; D: compound 12